Synchronizability and robustness of the large scale anatomical network of the Cerebral Cortex

Soós Bettina

2016/2017

Eötvös Lóránd University, Physics BSc

Consultant: Négyessy László

Synchronizability and robustness of the large scale anatomical network of the Cerebral Cortex

Acknowledgements

This work could not have been made without the support of some people, I want to say thank you in a few words.

I would like to thank to Négyessy László for the patient and persistent professional help throughout the birth of this composition and work, and along with Pollner Péter, I'm thankful to favor attention to my work at this busy time of the year.

I'm thankful to the people I met and experienced the inspiring conversations during my studies which helped me to keep focus on to the work I want to contribute to existence.

Not at least, I'm very thankful to my family for the support they gave me in every way they could.

Table of content

Introduction

The first part of this work will focus on how network analytic tools helped the understanding of the brain, more specifically the cerebral cortex functions. The second part of the introduction is to describe the mathematical basis of the tools mentioned in the first part and also those, which are relevant to our studies.

I. Biological aspects

I.1. Organization of the multilevel cerebral cortical circuitry: from neurons to regions

The complex network of the human brain especially the cerebral cortex is capable of performing simultaneously several functional tasks, such as learning, planning, storing and recalling memories, integrating information of the external word and many more [22]. A wealth of information has been gained about the biochemical functioning of the individual neurons, which establish the dynamic network of the brain by communicating via action potentials [22]. According to the neuron doctrine approximation, the functional unit of the brain is the neuron cell [12] [23]. However, the neuron doctrine has its limitations in explaining brain functions [23]. It e.g. cannot explain the irregular responding of neurons to repeated sensory stimuli and their spontaneous activity without stimuli, which is much better understood at the system level [45]. Accordingly, in recent neuroscience the emerging new paradigm is that neuronal ensembles rather than single neurons form the functional units of the brain [12]. This shift in paradigm about brain functioning calls for new approaches most notably he studying and analyzing neuronal networks. Considering the huge number of neurons, enormous amounts of functional neuronal connection combinations are possible, forming motifs to perform specific tasks in the brain and also in the cortex. In the cerebral cortex locally connected neuronal microcircuits modeled by the canonical microcircuit form the basic building blocks of the neural network [24]. These cortical microcircuits form columns, which are well known example of the neuronal connectome forming at a larger scale brain wide subnetworks of functionally connected neuronal clusters [24].A cortical column is vertically organized by locally interconnected neurons across the layers of the cortex. [25] [13]. The columnar organization is maintained by physiological mechanisms largely based on the afferent inflow signal. The cortical columns are prevalent throughout the cortex, as the columnar organization can be observed e.g. in the visual cortex, as in the auditory cortex, also in the higher order associational cortical areas. As shown in the sensory cortices columns represent elementary functional units and form a horizontal pattern of connections with other columns across all cortical areas. Underlining the limitation of the neuron doctrine at the higher levels of brain functions, neurons and columns of associational areas represent complex features combined by the simple features represented by the neurons at the lower level of brain functions as seen in case of the sensory systems [13]. However, apart from the local neighborhood restricted to a tiny brain or cortical tissue up to a cortical area, there is a huge gap in our knowledge in regard to the organization of the brain circuitry at the neuronal or even at the mesoscale population (columnar) level.

At the large-scale functions of the brain are studied by non-invasive techniques allowing full-brain scanning, which aid determining regional interactions comprising millions of neurons both at the structural and functional domains [26]. Functional neuro-imaging techniques are used to investigate brain area activation during cognitive tasks and resting state [27] [28]. Positron emission tomography (PET), and especially functional magnetic resonance imaging (fMRI) based on the recording of changes in blood flow and other metabolic demands, provide relatively good spatial

resolution. For high temporal resolution methods detecting electric and magnetic field changes are used, such that magnetoencephalography (MEG) or electroencephalography (EEG).

Depending on the methods used, different neural networks can be constructed. To determine physical connections between brain areas water molecule diffusion based techniques, such as diffusion tensor imaging (DTI) and related techniques can be used with magnetic resonance imaging (MRI) to localize the connecting axonal bundles of the white matter. The network reconstructed by using DTI is called ***anatomical network*** [26]**.** Combined with functional imaging during resting state or also in cognition, main cognitive networks involved e.g. in spatial attention, explicit memory (long term memory requiring conscious thoughts), object recognition, and in executive functions, the functional relationship between the activated brain regions could be mapped, thereby defining the so called ***functional and effective networks*** [26].

Physical connections can also be mapped via tract tracing [29]. It is an invasive technique, based on the capability of neurons to take up certain substances and transport into certain directions: either retrogradely from the axon terminals to the soma or anterogradely from the cell body towards the axon terminals. In case of bulk labeling, as opposed to injecting single cells or a small groups of them, tract tracing allows the mapping of directed connections between brain areas. However, in contrast to the imaging methods this technique also provides high spatial resolution at the level of single neurons or even synapses by allowing the reconstruction of single axonal fibers. Due to these advantages tract tracing is intensely used in the non-human primates to better understand the organizational features of the cortical circuits in the primate brain.

I.2. Networks of the brain

The first step to construct a network to analyze from the biological data, is to determine the nodes and the measure of association between the nodes giving the association matrix. Applying a threshold on the elements of the association matrix a binary matrix can be constructed, and can be used as the adjacency matrix of an unweighted graph. Network parameters then can be determined and analyzed. The magnitude of the threshold is related to the density and sparsity of the graph generated [14]. At EEG and MEG the nodes are the individual sensors or electrodes, but minimizing the covariance between the sensors is a condition often used. With the different methods of data acquisition one can get different types of connectivity, hence brain network. As mentioned above, s*tructural or anatomical connectivity* represents the neuronal, i.e. axonal connections, while *functional connectivity* uses the symmetrical statistical association or dependency between the nodes, for example correlations, coherence, and mutual information in their activity, which constructs undirected graphs. Mathematical models of *effective connectivity* between brain regions estimate the casual influence that each element exerts on the behavior of others. Thus, effective connectivity models, unlike many functional connectivity models, which are based on symmetrical measures of association, result directed networks to analyze [14] [26].

Most of our knowledge about the brain network originates from the results of studying the large scale cortical networks. This paragraph provides a short overview about these findings. In the cerebral cortex about 80% of the anatomical connectivity is formed within the areas. The remaining 20% inter-areal connection forms the large scale cortical network [32] .

Neuronal networks of the cortex show non-random connectivity and varying number of synaptic contacts with different synaptic strengths [16] [18]. Also recent observations of tract tracing studies indicate that at the large scale connection weights related to the number of synaptic contacts between areas has log-normal distribution and exhibit exponential decay with distance between two areas [16] [18]. The constraints of the spatial organization may have strong

contribution to the exponential distance rule [16]. Similar connectional density was found in the mouse whole-brain connectome datasets [16]. The connection density being in dependence with the spatial distance of the connected areas is corresponding again with the ***spatial embeddedness*** and with the cost of the long-range connections [16] [30]. Overall inter-areal connection density in graph theoretic terms (see in the II. paragraph) in the macaque cortex was 67% [16].

In the mammalian neocortex synaptic connections tend to be reciprocal [14]. Extensive studies in the macaque monkey suggest distributed and reciprocal connections between the identified cortical areas [31] [32] [13]. Similarly in the human, high proportion of reciprocal (bi-directional) connections are observed between cortical areas [2]. In the human motor cortex 75% of the effective connectivity connections were reciprocal, also it was shown that the proportion of reciprocal connections is decreasing with the distance of brain areas [2].

With the connection density and the reciprocity noted above, the cortical network, especially the structural, which has a large number of nodes forms a complex network, thus the understanding of the cortical networks requires exact network analytic tools [14] . Network theoretic tools, e.g. clustering measures, allow to determine properties, like the relative dense connectedness of close areas. For example, a clustering measure computed here is the Clustering Coefficient (see below) determines the proportion of triangle motifs in the network, can be used to quantify the connectedness of neighboring areas.

Structural connectivity places constraints on which functional interactions can occur in the network. Anatomically close areas share functional properties and are usually connected to each other [16]. Computational models offer methods to investigate the structure-function relationship. Empirically derived structural brain networks were used (e.g. the surface of the macaque cortex with 47 nodes) to simulate the dynamic behavior with physiologically motivated dynamic equations. The data from these simulations yielded the functional brain networks to analyze. Functional network with almost identical topological features to the anatomical network was derived on the long time-scale, while on shorter time samples or at high frequencies the functional networks were less correlating with the structural organization [14].

Analyzing community structure of fMRI functional networks showed functionally related brain regions to be densely interconnected with a relatively few connections between other clusters supporting the results derived from anatomical networks [14]. Accordingly, these functional features strongly depend on the clustering and convergence/divergence properties of the network elements, which largely determine their synchronization abilities.

Local connectedness is an abundant property of the dense cortical network in many scales [18]. According to the ***wiring cost*** constraint, wiring length should be globally minimized, using the shortest paths have evolutionary gain [30]. Spatial distance between brain areas have significance with signal transmission time and energy consumption. Also evolutionary pressure exist to build up fast communication, and keep material use low due to metabolic costs resulting in wiring length optimization [14]. It's a pressure to keep wiring length minimal, long connections are more vulnerable and have more expense metabolically. As it is a pressure to keep wiring length minimal, long connections are more vulnerable and have more expense metabolically. Studies on wiring length optimization by punishing physically long connections in the network showed that there are more optimal arrangements of the cortical areas. However, with the expense of some long pathways cortical network evolved to keep the average shortest paths in the brain minimal.

The wiring length minimization justifies the quantification of the the average shortest path (*ASP*, see below) during the network analysis of the cortex. Accordingly, *ASP* is important in determining the resilience of the cortical network and also in identifying the network indices best

characterizing the cortex.

Cortical hierarchy

Experimental studies provided compelling evidence in favor of the hierarchical organization of brain structure and function at the large scale [18] [31]. It is a major question how this hierarchy is represented at the level of networks, it is hard to catch the topological correlate of the realistic hierarchical organization of the brain.

Hierarchical signal propagation is known to be responsible for complex performances such as object recognition and cognition. Signal propagation in object recognition is starting from the hierarchically low ordered retinal receptor cells, then goes trough the visual areas reaching higher order cortical areas [30]. Between the higher order cortical areas and the primary sensory areas segregated bi-directional counter-stream pathways can be observed, thought to play feed-forward (FF) and feed-back (FB) signal transmitting roles in the cortical hierarchy [18] [34].

The physiological sign of the hierarchical organization is captured among others by the receptive field properties of neurons in areas at different levels of hierarchy [31] [35]. Generally, on the low hierarchical levels individual neurons have restricted receptive fields, with a characteristic feature specificity as e.g. the orientation tuning [22]. Some somato-sensory neurons sensitive to a certain skin area, providing a spatial representation of the body in the brain [22]. Higher order neurons, for example in the visual cortex, have large receptive fields, sometimes spanning the full visual field and react to more complex features of the stimuli as e.g. faces. Overall, progressively more complex receptive field properties observed in the hierarchically organized areas. However, it should be noted that the elaboration of the receptive field properties and therefore the information flow is not strictly sequential from the bottom to the highest levels of the cortical hierarchy. Instead, the areas form a complex network via their multiple interconnections with each other. Their influence on each other is substantially depend on the convergence and divergence of connections within the network of areas.

The application of network analytic tools, especially those related to the understanding of the convergence/divergence properties of the network elements are inevitable in understanding the hierarchical nature of the cortical organization and functioning. To identify the edges of hierarchy the measure of Convergence Degree (see below) is introduced here, and used to determine the role of these connections in the network robustness of the cortical organization.

The role of hierarchy in cortical processing

Dynamical models derived from structural data showed that low level early sensory areas showed transient responses, while higher associational areas, as the prefrontal cortex, integrate input over time with persistent activity, which makes it suitable for the more complex working memory and decision making processes [16].

Feed-forward pathways with sensory input assumed to have driving function in the network, while feed-back recurrent pathways might play modulator, regulator functions [18]. Axons with identified driving function showed faster conduction times and stronger synaptic activation than the modulatory connections. Reverse hierarchy theory suggest the initial role of higher order areas in the activation of the cortical network using categorical level representation for a quick identification of the input signals and match this activity pattern to that in the lower level areas to generate prediction error if necessary [36]. Related idea is the role of FB-FF circular connections is to resolve sensory ambiguity. The cortical inter-areal hierarchical organization and its interaction with local circuits thought to play role in predictive coding, while the prediction (expectation) signal descend, while the prediction errors ascend on the hierarchy network [16]. This model suggest the

perceptual processes depending on the expectation and experience of the perceiver [37]. Then the two types of perception, bottom-up (stimulus driven) and top-down (inference driven) can be distinguished and the internal representation is constructed both from the sensory input and the prior knowledge and FB connections are to disambiguate and explain the earlier representations. In this notion rather the unexpected features what signaled to the next stage of hierarchy, the function of FB and FF connections is to transmit the prediction and prediction error respectively. Mathematically prediction error can be expressed as free-energy principle, the “surprise” and the prediction/representation is adapted to minimize this quantity [38].

I.3. Synchrony: the fundamental characteristics of brain operation

Function

At zero or near-zero phase synchronization activity is modulated synchronously without temporal delay, or with delay much smaller than conduction times. Most neural synchronous activity fall into these categories [15]. Only very few and highly specialized models were able to account for zero lag synchrony in networks coupled with delay, which is substantial in neuronal networks due to e.g. conduction times, synaptic delays etc.

Mechanisms to zero-lag synchronization include entrainment trough common drive from a single source. Some cortical and sub-cortical areas or in local networks pacemaker cells may can serve sources like that [15]. It is important to note the limitations of a common drive, since an entrainment like that determines both the rhythm and synchronization among the target cells [15]. This entrainment via an auxiliary hub can always, with an addition of a lower bound to the coupling strength, can synchronize activity for any other arbitrary coupling. The minimal coupling strength were found to be the function of the type of coupling between the hub and the network, but also dependent on the network properties. So modifying these factors allow a a dynamic synchronization process [15].

In addition to a common input synchrony can also emerge via convergence of the inputs to a common target. Interestingly, in the cerebral cortex divergent branches of axons of the different, even neighboring neurons typically do not converge on the same target regions [18]. Accordingly, neuronal synchronization fundamentally depends on the convergence/divergence of the cortical connections. Although, it is known that connections in the cortex are not randomly arranged, the understanding how convergence/divergence is organized is not clear.

Network robustness and synchronizability are strongly linked as it is known from spectral graph theoretic approaches. Using the targeted attack procedure, we will show how different network indices affect these features.

Fast brain synchronization and to keep the synchronization sufficiently long time is important for proper functioning. The synchronous activity in the brain network can be modeled with coupled oscillators (see below at II.3.), but it is hard to provide consistent data from the dynamical processing. The different functioning of the brain can be viewed as the special synchronized states varying in time [39].

In this work the robustness of the cortical synchronization properties trough the spectral analysis of the connection matrices derived from structural data are examined by convergence/divergence related attack strategies, to analyze the relation of signal convergence/divergence and synchronization.

The role of synchronous activities in the brain

Synchronous activation of brain areas or neuronal groups is widely observed on different scales of the neural organization. Oscillatory timing is important in neural plasticity with forming functional motifs by enhancing connections promoting the coherent firing couplings [3]. Neural synchronization may give the answer to the question, how the brain is able to process numerous computation simultaneously in spatially segregated areas [39]. Phase-locked high frequency oscillations may span the spatially distinct brain regions [14]. Phase locking synchronization between distant neuronal assemblies e.g. during feature binding support these ideas [15].

Recordings in human subject supports the relation between the shorter wavelength synchronous oscillatory activity during a variety of cognitive functions. Synchrony of distributed neural discharges establish temporal relations by systematic phase-lag. In the debated model of neural synchrony as contextual framework sensory stimuli interact with internally generated signals for building up predictions about the world. They suspect oscillatory responses to be linked to general cognitive functions as selective attention, short- and long-term memory and multi-sensory integration [15].

Physiology and dynamics

Coherent periodic activations provides a temporal window to the ongoing firings on the phase of the oscillation [39] [40]. A couple of neural groups are able to communicate if they're in an excitable state at the time their signals meet. These requirements meet if two oscillating elements are phase-locked [8]. There is phase-lock properties e.g. inside the cortical areas around the gamma-frequency range (30-100 Hz) and between cortical areas in the beta-frequency range (15-25 Hz) or lower [8]. Phase-locking should be present in a selective manner, modifying coherence of brain areas is a need in cognitive flexibility to switch functional tasks, global or irregularly high proportion of phase-locking is pathologic, can be observed during epilepsy [8]. Slower frequency ranges are also prominent in large-scale network dynamics, alpha rhythms around 10 Hz, theta between 4 and 8, and the delta is around between 1 to 3 Hz [8]. Possibly oscillation coherence have a role on selective attention by phase-locking to the preferred stimuli [8]. Inverse correlation between the frequency of oscillation and the distance of the synchronous activity was found [3].

Cellular functional networks exhibit transient synchronization, and perform metastable dynamic changes in less than 1s time scales [14]. This suggests that fast changes in functional linkages are made possible by the underlying pattern of connectivity of the brain. However, the relevant network features at the large scale are unclear. While the brain activity shows spontaneous fluctuations the functional networks form robust resting state phases, which is a non-random pattern of activity based on the interaction of a define set of areas [14].

In the brain zero-lag synchronization is arising from the interaction of the excitatory and inhibitory neurons [15] [8]. Fast oscillations can be the result of the instantaneous, electrical gap junction coupling of the inhibitory neurons making the connected inhibitory subnetwork highly synchronous. As the consequence, this will result in the synchronous activity of the principal excitatory cells in the cerebral cortex. If both electrical and synaptic couplings present weakly they show similar behavior and add up linearly. But probably more than one mechanism contribute and impact the dynamic zero-lag synchronization process. At a larger scale it is suggested that reciprocal coupling of cortical areas with the different thalamic nuclei may support the coordination of distributed cortical processing [15]. The divergent reciprocal connectivity of thalamic cell groups to different cortical neuronal populations could redistribute ongoing cortical activity and synchrony. It was shown that this configuration to support zero phase lag synchronization for any conduction delay [15]. In this case the central element is key for the communication, but does not dictate the

dynamics [15].

If the oscillation is present with consistent phase difference one can talk about near-zero lag synchronization [15]. The relative phase difference can take place due to the relative delay to the global synchronized dynamics. A possible explanation of near-zero lag synchrony is detuning, which is ensued from the heterogeneity of the oscillating elements, which have intrinsically differing properties, such as different resonant frequencies [15]. Phase differences also serve as temporal code in brain information processing [15]. Coding mechanisms based on phase lag has been observed in the theta (4-8 Hz) range in the hippocampus and in the gamma range (>40 Hz) in the neocortex. These oscillations are seem to be generated by internal mechanisms independently of the stimulus timing. Furthermore, oscillation in the theta frequency range are also observed in the neocortex where they coexist with faster oscillations [15].

Two ways of synchronous temporal information coding about stimuli are proposed. One is that the modulation of the strength of synchronization serves as signal information about the relatedness of e.g. the visual features that activate those neurons, the so called binding [15]. A second way of coding is stood in the phase differences or delays among the participating neurons and similar to what can be observed in the hippocampus [15]. In the neocortex neurons are rarely synchronized with exact zero delays. These delays are up to ~15ms scale and do not reflect conduction delay as they vary as a function of stimulus properties [15]. A major question is how the convergence/divergence properties of the cortical network determine these oscillatory properties and the synchronous dynamics.

I.4. Vulnerability of brain networks

Synaptic connections of neurons are shows *plasticity* and can be altered by the learning rules of the brain [12]. The network of neuron assemble is capable of changing its connection pattern over time. It has an effect on the formation of memory trough learning and can compensate impaired connections. The brain stays functional and show plasticity to small damage, like to damage in the axons, which are known to be highly vulnerable to injury.

Structural and functional connectivity in cellular networks undergo dynamic changes. In general, structural rewiring takes longer than the time needed for changes in synaptic strengths, but the degree and time scale of synaptic connectivity changes is debated [17] [41]. Regarding functional connectivity, where spontaneous fluctuations are observed and the network is highly responsive to perturbations on the time scale of hundreds of milliseconds induced by e.g sensory input or cognitive tasks. Though on longer timescales, from seconds to minutes, functional networks also tend to show *robustness* [14].

However, the flexibility and rearrangement of large scale neural pathways is not significant in normal circumstances only in case of lesion and in the long time scales [17] [41]. A striking example of neural plasticity is resulted by sensory deprivation, when a route of sensory input is impaired and the brain network undergoes reorganization resulting in changes of cortical functions as e.g. seen in early blind subjects whose visual cortex becomes responsive to other sensory modalities like touch and hearing [17]. Primary sensory cortices associated with the deprived modality became governed by the remaining modalities, the phenomena called cross-modal plasticity. Plastic changes vary widely across brain systems giving rise to specific alterations. This process results in increased spine and neuron density in the auditory cortex after deprivation of other modalities in rats and mice [17]. It was found that plastic changes lack the effects on absolute sensitivity of the remaining modalities, instead it led to differences in performance on more complex tasks [17]. The cerebral cortex play primary role in these compensatory changes [17]. Growing evidence suggest that after sensory deprivation the reorganization of polymodal

associational areas are mediated by mechanisms similar to those that operate during normal development, such that the competition between different inputs [17]. Human studies showed posterior visual areas being active during somato-sensory processing in blind and similar results were shown to the other modalities [17].

Reorganization of connections might be due to alteration in local connectivity or due to alterations of long-range sub-cortical connectivity, however the latter seem to be limited to the development or takes place in very long time span in adults [17] [41]. The removal of sub-cortical connections do less harm in the developing organism as opposed to that in adulthood.

Feed-back pathways seem play significant role in the reorganization of connections e.g. in cross-modal plasticity. These type of rearrangements seem to be more likely to be modifiable even in adulthood. [17]

Some neural systems, like word and object recognition, do not seem to be constrained by sensitive periods of development and can be modified throughout lifetime [17]. Altogether, it is a major questions which are the major areas and connections involved in these compensatory changes in the brain.

Pathological cortical organizations

Abnormalities in neural structure and synchrony were shown in some symptoms of psychiatric disorders, like schizophrenia and Autism Spectrum Disorder [15]. In schizophrenic patients the reduction in phase-locking of oscillations in the beta and gamma band can be observed [15]. Also it is suggested that the abnormal generation of internal experiences (positive symptoms: illusions, hallucinations etc.) are related to increased beta and gamma activity and it is associated with enhanced white matter connectivity in temporal regions of the cortex. Patients with autism spectrum disorder show reduced functional connectivity throughout the cortical language system and they also showed reduced neural synchrony [15].

To determine the structural robustness, i.e. the connectedness of the cortical network, and the synchronizability, network analytic tools were used. Among other methods to investigate vulnerability and the support of synchronous dynamics in the system, spectral analyses of the special connection matrix of the brain network, the Laplacian (see below), were performed. Combined with other measures like the nr. of connected components in the network, the vulnerability and the measures of vulnerability can be analyzed.

II. Network analyses

II.1. The structural and functional organization of complex systems

Network analyses is aimed to uncover functionally meaningful structural properties of complex systems with numerous interrelated components. Analysis of real world or artificial networks is based on graph theoretic tools. In the following part of this section some of the major indices used in network analyses will be introduced.

Network representation of complex systems

A graph G(V,E) is the set of vertices *V,* and their set of connections, the edges, *E*. Thus, an

edge is described with a pair of nodes E → (V_1,V_2), if the order of nodes in the assignment is irrelevant, the graph is undirected, and it is directed otherwise. Self-loops are edges that connect a vertex to itself. Multiedges are repeated edges between the same pair of nodes. Furthermore only graphs without self-loops or multiedges will be considered. As independent of the physical distance between the connecting elements a graphs are considered to be topological objects. Graph topology can be described with a varieties of measures.

A convenient way to describe graph topology is with matrix representation, and it can be generated by several ways. The *Incidence matrix*, I_{ij}, is a NxM dimensional matrix, where N is the number of vertices and M is that of the edges. The entry I_{ij} is 1 if node i incident in edge j, 0 otherwise. Every column in I_{ij} has two entries, because each edge is connecting to two vertices.
If the graph is directed, distinction of head and tail nodes can be made as an edge leaving the node it takes the value 1 and -1 if it's arriving to it.
In I_{ij} 2M non-zero elements are stored on N*M digits.

Another way of matrix representation is with the ***adjacency matrix*** A_{ij}, where both matrix indexes representing the same set of nodes so A_{ij} is a square matrix. It's elements in the presence of edges between I and j is 1, and 0 if I and j not connected. In the case of undirected graphs the order of the indexes are irrelevant, $A_{ij}=A_{ji}$, the adjacency matrix is symmetric. If the graph is directed A_{ij} represents an edge coming from i to j. In a graph without self-loops the main diagonal elements A_{ii} don't carry information about the graph, since it is known it is always 0. The adjacency matrix can be expanded by filling in these, only vertex specific diagonal places.

The *degree matrix* D_{ij} is a diagonal matrix, where the non-zero elements at i=j represents the degree of vertex i.

Laplacian matrix **L**=**D**-**A** for a directed network **D** with containing the out-degrees will preserve the row sum of the Laplacian to be zero. Notice the connection between the Laplacian and the Incidence matrix for undirected graphs,

$$\boldsymbol{I}\cdot\boldsymbol{I}^{T}=\boldsymbol{L}$$

The usefulness of these different matrix forms will be shown later.

Network properties

General characteristics

Network *density* is the ratio of existing edges to all the possible edges, and can be calculated by

$$\eta=\frac{|E|}{|V|\cdot(|V|-1)}$$

Density is often related with the physical cost of the network, as seen for example in the brain with more edges requiring higher the metabolic demands [14].

The *reciprocity,* also called *cohesion index*, of a directed graph is given by the proportion of bidirectional connections to all connections in the graph. It gives the probability, that a chosen edge has a connection existing in the other direction as well. Importantly, the cortical network is highly reciprocal, but there are non-reciprocated connections as well, which makes the total network directed (especially in its binary representation).
Reciprocity can be calculated by the element-wise product of the adjacency matrix and it is transpose, $\mathbf{T}=\mathbf{A}.*\mathbf{A}^{T}$. The proportion of the sum of all elements of **T** and the sum of the adjacency matrix elements quantifies the reciprocity.

The number of connections a vertex has is the ***degree*** (k_i). In the case of directed graphs we can make a difference between incoming and outgoing edges, so then we can define the *in-degree* and *out-degree* of *a* vertex.
With matrix representation the degree can be expressed as,

$$k_i = \sum_{j=1}^{n} A_{ij}$$

which formula, if A_{ij} is the adjacency matrix of a directed graph, gives the in-degree of the graph. The out-degree can be calculated by summing columns of A.
High degree nodes are often considered to play important roles in the network, those kind of nodes are called the *hubs*.

The *net flow,* is the in-degree minus the out-degree. It resembles the direction of local information flow through the node. By applying it to an edge e=i → j it can be defined as the in-degree of node i minus the out-degree of node j.

A basic topological characterization of a graph is its ***degree distribution***, which be defined by the number of vertices having a certain degree. For comparability across different networks the degree is usually normalized with the number of vertices in the graph.
The degree distribution is useful to identify the different kind of network topologies. For some example, in a random network, where all connections are equally probable the result is a symmetrically centered Gaussian distribution. Another noted degree distribution called the scale-free, which follows a power-law distribution [14].

Assortativity gives the correlation of the node degrees: positive assortativity means that the high degree nodes tend to connect with nodes of high degrees as well [14].

A path can be described as a sequence of connected vertices and edges without repetition. The length of these paths is the number of edges in it. The *shortest paths* (sp_{ij}) of pairs of nodes can be determined, it is also called the *geodesics.*

If there is an edge from the end node to the starting node of the path, it is addressed as a *cycle* with the order of the path length plus one. An element of the k matrix product of the adjacency matrix A^k_{ij} gives the number of k length walks between vertex i and j. The trace of the k matrix product, $tr(A^k)=\Sigma_i A^k_{ii}$ gives the number of k-cycles in the graph multiplied by k, because all cycles are counted k times with every node in it. In the case of undirected paths it is also multiplied with two, because the two directions are identical.

In the brain shortest paths play an important role in transport and communication within a network. Because wiring length should be globally minimized, using the shortest paths have evolutionary gain. Information processing in the first order is expected to be fast, and the fastest way of travel is trough the shortest paths. The nature of information spreading on these routes may important to functional processing in the brain, longer path can be useful e.g. after damage providing adaptive features in the brain.

An important characteristics of network is the ***average shortest path length***, asp, or *characteristic path length,*

$$asp = \frac{\sum_{i=1}^{|V|} \sum_{i \neq j=1}^{|V|} sp_{ij}}{|V| \cdot (|V|-1)}$$

It’s important to note that the above definition is only giving sensible values if the graph is connected. It’s possible to manage the asp for disconnected graph if we only consider paths between the connected components, or giving the disconnected pairs of nodes an artificial high sp value, e.g. |V|-1 is the highest possible sp value in a graph.

The average shortest path length describes how fast is the signal propagation in a graph, with other words it describes the *efficiency* of the information transfer in the graph. The relationship is inverse, as networks with small asp-s have high efficiency [14] [9]. Random networks, and many real-world complex networks, like the brain, have small average shortest paths, while regular lattices possess high asp values [14]. Asp changes mostly logarithmically as a function of the network size [9]. The ***diameter*** is the length of the longest shortest path.

In the brain ASP can describe the level of global integration and is a measure of global connectivity. Small ASP means distributed/integrated information processing. ASP have an inverse relation with the efficiency of parallel information processing, a property important in the brain functioning [46]. Due to energy (metabolic) cost minimizing in the brain ASP minimizing is demanded. Thus, the investigation of the ASP and it as a vulnerability measure is a good method of analyzing the brain function.

An undirected graph is *connected*, if there's a path between every pair of nodes. In a directed graphs, if a directed or undirected path exist between all pairs of vertices, the graph is ***weakly connected***. If there's a directed path between every pairs of nodes in both direction, than the graph is ***strongly connected***. The number of weakly connected components can only be smaller or equal to the nr. of strongly connected components because if a network is strongly connected, than it is also weakly connected. If a graph is *weakly connected* can be determined from it is connectivity matrix. A directed graph looses weak connectivity when the undirected graph constructed by considering its directed edges undirected becomes unconnected. If a graph is strongly connected, there exist an at least k=|V|-1 length of path from all vertex i to j, therefore all i!=j entry of the $\Sigma_k(A^k)_{ij}$ should be non-zero.

The c*lustering coefficient*, also known as *transitivity*, a local measure (cc_i) if it is the proportion of the connected nearest neighbors of a node to all the possible connections varieties of the neighbors [14] [9].

The global ***clustering coefficient*** (CC) provides the probability that two neighboring nodes of the same node are also adjacent. It gives information about the proportion of cycles with the length of three, which can be quantified as the ratio of the triangles to all possible connected triples. It will be shown that the adjacency matrix and also the local Overlapping of an edges can be used to give the number of 3-cycles.

Random networks have low clustering coefficient compared to many real-world networks, like the brain, where the interaction of neighboring nodes supports the local information transfer efficiency [14].

CC, as the describing the presence of the triangle motifs in a graph, is a measure of local connectivity and useful to quantify clustering, e.g. in brain networks, where clustering is compatible with segregated/modular processing. It is known that neighboring cortical areas innervate each other, while distant areas are less likely to be connected [46]. Also, wiring cost minimizing of the brain is related to maximizing clustering, thus its a good measure to describe a part of brain functionality. CC is also related to the local efficiency of fault tolerance [46], suggesting it to be a good quantity of vulnerability.

Centrality, the importance of network elements

Centrality measures allow us to determine the relative importance of an edge or a node in the network. Node centrality measure for example the degree, but also the closeness centrality giving the (reciprocal of the) average geodesic length from a vertex to every other [19]. Betweenness centrality, highlighted below, measuring the fraction of geodesics from all which a vertex takes part in [19]. Betweenness centralities are important measure of the control a network element exerts on the information flow if we assume information flows on the shortest possible paths.

While degree centrality is a local measure of the network quantities employing the shortest paths, like the *edge betweenness* and the *convergence degree*, detailed below, are the function of global structural properties.

Edge betweenness ($EB_{e)}$ is the measure of how important an edge is by considering the amount of shortest paths going through it.

$$EB_e = \sum_{k=1}^{|V|} \sum_{k \neq l=1}^{|V|} \frac{{}^{e}m_{kl}^{sp}}{m_{kl}^{sp}}$$

where ${}^{e}m^{sp}_{kl}$ is the is the number of geodesics between node k and l going trough the edge e, and m^{sp}_{kl} is the number of any shortest paths between k and l.

Convergence/divergence of connections is an important part of network functioning, but it describes local signal propagation. By considering the convergence of shortest paths in a measure of global structural properties can be made.

Convergence Degree

This chapter is based strongly on the findings in [4].

CD_e defines the convergence or divergence of the shortest paths going trough an edge. Let In_e be the set of vertices starting the path in sp_e, and Out_e be the set of the arriving vertices. Notice, that In_e and Out_e can be defined only on directed graphs, since the directionality of e is required, otherwise In and Out is identical. If e is part of a chorless cycle, In_e and Out_e may overlap, so lets define $Ovl_e = In_e \cap Out_e$ and $SIn_e = In_e \backslash Ovl_e$ and $SOut_e = Out_e \backslash Ovl_e$.

It is also possible to determine a less global version of these sets, if we restrict sp_e based on it is natural stratification in respect to the distance of the node from the e edge. Without the overlapping areas, this builds up a tree-like structure with the roots being the incoming shortest paths, the stem is the edge, and the outgoing shortest paths making up the branches of areas reached by the signal transmitted by e. Connections between different strata are not allowed, because it would alter the shortest paths. If only the first neighbors are used in sp_e, the cardinality of In_e, $|In_{e=ij}|$, gives the in-degree of node i, $|Out_{e=ij}|$ is the out-degree of j, $|Ovl_e|$ is the number of 3-cycles that edge e the part of, thus it is related to the clustering coefficient. The node i in e=i->j is the only part of the zeroth strata of In_e, and j in the zeroth strata of Out_e respectively. The local convergence degree using up to the first strata gives the net flow of an edge.

To eliminate the dependence of the network size, the measures SIn_e and $SOut_e$ are determined relative to all amount of vertices participated in shortest paths going through e. The normalizing factors then, |SIn U SOut U Ovl| = |In U Out|, and

$$RIn = \frac{|SIn|}{|In \cup Out|} \qquad ROut = \frac{|SOut|}{|In \cup Out|} \qquad ROvl = \frac{|Ovl|}{|In \cup Out|}$$

$ROvl_e$ is the *Relative Overlapping Set* of edge e, often just referred as the *Overlapping*. Then, the Covergence Degree can be defined as $CD_e = RIn_e - ROut_e$.

CD value close to -1 means that the edge injects information from small amount of node to wide range of areas, the edge disperses the sign going through it. Edges with CD value close to 1 means it integrates the sign arrived from extended range of nodes, and transmit it to fewer others. High Overlapping means, the edge mostly transmit sign in feedback cycles setting up the reverberation of information. An edge to have a non-empty Overlapping Set it is necessary be on a chordless cycle. The relationship of CD and Ovl can be formulated with $|CD|<1-ROvl$. Note, that in this form ROvl is analogous to the Jaccard coefficient, the value used to determine similarity of sets.

The sum of the Convergence Degree of all edges describes an average ejected signal how will travel trough the graph in the long time scale. Positive CD sum means the graph rather absorbs the information going trough it, negative CD sum indicates the graph overall disperses the signal ejected into. The normalized version of the CD sum is the average CD of the edges, the *Average Convergence Degree*.

As EB of an edge is proportional to the amount of shortest paths going trough an edge, this increases |InUOut|, but since CD is normalized with this factor high EB do not indicates high CD. CD and edge-betweenness are uncorrelated and therefore independent edge-based measures [8].

Node reduced CD flow

To represent information flow properties trough nodes, the node reduced Convergence Degree was constructed. It' based on separating both the incoming and outgoing edges of a node by the sign of their CD to positive (convergent) and negative (divergent) and sum it to

$$^{\text{in}}\sigma_i^+ = \sum_{j=1}^{d_{\text{in}}} CD_{ji} \qquad ^{out}\sigma_i^+ = \sum_{j=1}^{d_{out}} CD_{ij}$$

if CD > 0, and

$$^{\text{in}}\sigma_i^- = \sum_{j=1}^{d_{\text{in}}} CD_{ji} \qquad ^{out}\sigma_i^- = \sum_{j=1}^{d_{out}} CD_{ij}$$

if CD < 0.
Then the CD flow Φ(i) is written as,

$$\Phi_i = {}^{\text{in}}\sigma_i^+ + {}^{out}\sigma_i^+ + {}^{\text{in}}\sigma_i^- + {}^{out}\sigma_i^-$$

II.2. *Characteristics of network architectures and topologies*

It is general to compare the parameters of the analyzed networks with the (null) distribution of equivalent parameters estimated in random networks with the same nr. of nodes and edges, thus analyzing random networks is important to determine the characteristics of complex systems.

Random neworks

An *Erdős-Rényi random graph (ER) (Bernoulli random graphs)* is a graph constructed with even independent probabilities *p* to every edge in the graph to exist [19].Constructing networks with this method gives a phase transition at $p_c=1/n$, where above the critical p values a connected component forms with the size dependent of n, while below p_c small groups of vertices remains unconnected independent of n [19] [9]. Other method of construction is adding edges between evenly chosen pair of nodes, until a desired number of edges reached.

The average degree of an ER graph can be formulated by <k>=p*(n-1) [19].

Estimating the diameter, the average shortest path length, and the clustering coefficient is possible in the case of sufficiently high mean degree providing enough connection density at n*p>=ln(n), with the following forms [9].

$$diam = \frac{\ln(n)}{\ln(p \cdot n)} \qquad asp \sim diam \qquad C = \frac{p \cdot k(k-1)}{2} \cdot \frac{2}{k(k-1)} = p = \frac{\langle k \rangle}{n}$$

The number of edges present,

$$m \sim \binom{n}{2} \cdot p$$

The ER graph has Binomial degree distribution,

$$Pb(k) = \binom{n-1}{k} \cdot p^k \cdot (1-p)^{n-1-k}$$

Than the expected value of the degree can be given with $\langle x \rangle = \Sigma_x x P(x)$, and with the use of the derivate of the binomial formula

$$n(a+b)^{n-1} = \sum_{m=0}^{n} \frac{m}{a} \binom{n}{m} a^m \cdot b^{n-m}$$

substituting b=1-a, the form of the expected value turns up in the equation n=<k>/p, so the mean degree expressed as <k>=n*p, which for sufficiently large n corresponds to the previously stated <k>.

For large N and fixed <k> the degree distribution is well approximated with the Poisson degree distribution [9],

$$Pp(k) = e^{-\langle k \rangle} \frac{\langle k \rangle^k}{k!}$$

For a ER graph with large number of nodes, and in the limit of large mean degree <k>, e.g. dense graphs, the Binomial degree distribution tends to the Gaussian degree-distribution [14].

$$Pg(k) = \frac{1}{\sqrt{2\pi \langle k \rangle}} \cdot e^{\frac{-(k-\langle k \rangle)^2}{2\langle k \rangle}}$$

It is possible to construct a graph with arbitrary degree-distribution with having the set of nodes having certain degrees noted with half connections on each, called the studs. Then one can connect a studs with evenly choosing two to connect until all the connections established [19]. This method is resembles to another method of graph construction with arbitrary degree-distribution, in which with rewiring a predefined graph with sufficiently enough steps, by exchanging edges without generating multiple edges or self-loops. The method will give a randomized graph with a distinct degree-distribution.

The clustering coefficient can be estimated to a random graph with arbitrary degree-distribution with the average <d> and deviation of the degrees σ_d in the following way,

$$C = \frac{\langle d \rangle}{N}\left[\frac{\langle d^2 \rangle - \langle d \rangle}{\langle d \rangle^2}\right]^2 = \frac{\langle d \rangle}{N}\left[\left(\frac{\sigma_d}{\langle d \rangle}\right)^2 - \frac{\langle d \rangle - 1}{\langle d \rangle}\right]^2$$

Natural networks typically reveal different regime of properties than what is seen at artificially generated random networks. Different categories of network topologies can be determined by these coherent set of properties.

Small-world properties

In natural networks the combination of small average shortest path length and high clustering is frequently observed, placing high proportion of natural graphs into the regime of small-word networks. Small-world graphs are intermediate between regular lattices and random graphs. They possess significantly smaller average shortest path lengths than a regular lattice with similar clustering and show high clustering compared to a random graph with the same asp [14] [9]. Small-world properties help efficient communication between the elements, in a D dimensioned lattice the average nr. of vertices needed to pass by in order to reach an arbitrary chosen node grows with the lattice size as $N^{1/D}$. Related to asp, with the logarithmical dependence on the network size in SW graphs this stays small even at high number of nodes [9]. A specific approach to characterize the natural small-world properties is defining the level of clustering with the clustering coefficient, its proportion to the average shortest path length gives the measure of global efficiency. Economical small-word topology denotes small-world features, but with the relatively low local connection densities, referring to the 'cost' natural networks often have to support their connections [14]. However, it is important to differentiate the origin of small-world properties, as dense networks may hold short path length and high clustering trough the high connection density, so the small-world property may arise from the high density instead of being an independent property of the network topology [18]->[15].

Spatially embedded networks should minimize long range connections while keeping efficient communication, thus small-word organization should be a suitable topology for those. Furthermore, in the face of signal propagation, SW network are suitable to optimize the integration and segregation of the transmitting sign [42] [43] [44].

By the analyses of species-specific connection matrices, e.g. macaque visual cortex, cat thalamo-cortical systems, sets high clustering of functionally related areas with small average shortest path length, suggesting the small-word properties of the network, but furthermore, with the low connection densities of the long-range connections in the macaque monkey, the small-world topological feature proposed is rather considered economical small-word organization [14]. Also,

mapping of the structural networks of the human brain show small-world architecture and revealed significant overlap between anatomical network modules and the functional systems in the cortex [14].

The small-world network architecture parallel supports segregated (with high clustering) and distributed (with small ASP) information processing and is a suitable topology for dynamic complexity [46]. By minimizing wiring and energy costs simultaneously and show high slobal and local efficiency with low cost [46], SW topology seems to be a applicable organization to the brain network, and worth to investigate.

Scale-free networks

Scale-free networks are special to the the heterogeneity of node degrees. A SF network is abundant with nodes of small degree and have a few nodes of high degrees. The degree distribution of a SF network power law correspondence, $p(d) \sim 1/d^{\alpha}$, often in biological networks with the exponent $2<\alpha<3$. The distribution has the property of $f(a*x)=b*f(x)$, thus rescaling the function on the x axis won't result structural change, it is scale-free [9]. This topology is present in many natural networks, like the Internet and the World Wide Web, and it is often related to growing networks with preferential attachment, which means that choosing a connection partner to a node is not evenly distributed, but nodes connect with higher probability to high-degree nodes [19][14].

High degree nodes are constrained in spatially embedded networks since the number of edges, that can be connected to a node is limited by the physical space [9]. Furthermore connection cost limits having high degree nodes, thus network with these properties posses and altered power-low degree-distribution, called exponentially truncated power-law degree-distribution [14].

Structural and functional networks of the brain shows scale-free-like properties [7]. Macaque and cat functional networks was found to exhibit exponentially truncated power-law degree distribution, and highlighted the high degree characteristics of the multi-modal association cortical areas [14].

Network architectures subserving hierarchically organized parallel distributed processing

Convergence and divergence of lines of information transfer probably plays important role in how the brain select input signals for further information processing [15]. It characterizes segregation (working on different specific tasks in parallel, e.g. elementary features of an object) and integration (integrating or binding related information processed in parallel circuits) which are fundamental parts of the brain and especially cortical functions. *Integrity* of a network architecture by the combination and integration of signals related to the convergent properties of the signal flow, while s*egregation* can be associated with the divergence of the routes of signal transfer. Control properties associated with recurrent information processing, with connections being part of loops and cycles, related to the overlapping of information.

As divergent edges spread information from smaller to larger amount of areas, these kind of connections can play a role in adjusting node activation and enhancing synchronization with transferring effects to high proportion of areas. Determining connections based on the convergence and divergence of signal flow and integrate it on nodes can be useful to build up the hierarchical organization of brain areas. Neural network circularity also plays significant role in the information processing, chord-less circles gives information about signal reverberation, measures used here with the overlapping of shortest paths may help to uncover this property as well.

If nodes contribute to the network dynamics differently asymmetry in signal processing emerge, information propagation have a global direction, a hierarchical ranking of network elements can be made. Hierarchy can be observed in many self-organized and evolutionary propagated networks. It is a global structural feature of the dynamic network function. However to detect and distinguish different forms of hierarchies is a difficult task as in many networks due to connections against the flow of hierarchy, e.g. laminar or backward, are often present [20].

To determine hierarchy in [5] the proportion of edges, which is not part of any cycles is used. In [20] the proportion of the number of nodes reachable were determined as the rank of hierarchy. And [6] uses the convergence/divergence of edges leaving and terminating a node to determine its hierarchical level. Because edges having non-zero Overlapping needs to be on a cycle, and an edge with higher Overlapping posses smaller absolute CD, due to the normalization, these quantities can be used to identify the hierarchies in a network. However hierarchy is not always obvious specially in the case of complex networks. Asymmetry in node connections, the condition needed for hierarchy, are often disrupted with cycles and backward connections [5] . In the brain feed-back and feed-forward connections, even if in the binary matrix representation show symmetry, the connections reveal functional differences, thus the asymmetry needed for hierarchical categorizing is present.

Hierarchy can be built up through the shortest paths. Related property the Convergence Degree, especially the integrated edge CD can be used to determine the hierarchical organization. Lower order areas performing information source, segregating functions, which is supported by divergent outgoing edges. Higher order areas receiving signal trough this divergent feed-forward connections from the lower areas and provide convergent feed-back, this performs information sinking to the lower areas [4]. Representing nodes on a two dimensional coordinate system of the CD flow, with the x axis being the incoming σ, the y axis the outgoing σ, every node gets plotted separately in every quadrant representing different convergent characteristics of the input/output combinations (-in/-out, +in/+out, +in/-out, -in/+out), and by analyzing the placement of the nodes, the type of information flow it posses preferably can be determined. See figure 5. in [6]. The upper left quadrant by giving the amount of divergent incoming edges combined with convergent outgoing ones, tells about the information sinking nature of the node, related to allocating or boardcasting properties. The lower right quadrant describes the amount of convergent incoming and divergent outgoing edges the node have, the node is provides/injects information to the network, therefore serves as a source of information. The lower left and upper right parts corresponding to divergent and convergent relay properties.

In real world network, specially in neural network, nodes tend to place around y=1/x curve in the bottom left, top right “relay” quadrants, and around the y=-x curve in the top left, bottom right quadrants. The negative correlation of the CD with the incoming and outgoing edges is pronounced, meaning the typical opposing CD sign of the efferents and afferents (i.e. reciprocal connections) of an area. Cortical networks typically posses less router or “relay” nodes, possibly due to high evolutionary costs compared to the strength of functionality [4] [6].

II.3. Spectral analysis and network dynamics

Spectral graph theory

The set eigenvalues μ_i i=1..n, where n=|V|, of the adjacency matrix of G is often called the spectrum of G and along with the eigenvalues λ_i of the Laplacian matrix important consequences about the network structure and function can be deduced. The following section we use to summarize some spectral properties of A and L related to our studies.

If the graph is undirected A and L is symmetrical, therefore it's eigenvalues are real and the corresponding eigenvectors are orthogonal. If G is directed the eigenvalues can have imaginary part [9], but the assumption of matrices with high reciprocity standing close to undirected matrices with small imaginary parts can be investigated . If A and L are a reducible matrices, than the corresponding matrix is not strongly connected.

The number of distinct eigenvalues of the adjacency matrix A is an upper bound for the diameter of G [9].

The Perron-Frobenius theorem states, that an irreducible non-negative matrix A (as the adjacency matrix of a connected graph) have an eigenvalue μ_N, with the multiplicity of one, such that $|\mu| < \mu_N$ holds for all eigenvalues μ of A. The value of μ_N can only decrease when vertices or edges are removed from the graph [9].

It's been shown though the Perron-Frobenius theorem, that the second smallest eigenvalue, the *algebraic connectivity*, λ_2 of the symmetric Laplacian matrix L, is zero if and only if the corresponding graph is not connected. And that removing edges from an undirected graph can not increase λ_2.

By Courant's theorem the second smallest eigenvalue of a positive semidefinite matrix with a row-sums zero can be expressed as,

$$\lambda_2 = \min_x \vec{x}^T \boldsymbol{L} \vec{x}$$

where x is all the column vectors perpendicular to the vector $[1,1,1,\ldots,1]^T$, while the largest eigenvalue is proved to be,

$$\lambda_N = \max_x \vec{x}^T \boldsymbol{L} \vec{x}$$

Upper bounds of λ_2 are possible to determine with the size of the vertex set $|V|=n$ with the minimal degree k^{min} or with the size of the vertex and edge set $|E|=m$ in the following form,

$$\lambda_2 \leqslant \frac{n}{n-1} k^{min} \leqslant \frac{2 \cdot m}{n-1}$$

Its shown, that λ_N can not increase by removing elements of the graph, and is bounded by,

$$\frac{n}{n-1} k^{max} \leqslant \lambda_N \leqslant 2 \cdot k^{max}$$

Furthermore let's consider the vertex connectivity *vc* and edge connectivity *ec*, as the minimal number of vertices and edges needed to remove to disconnect the graph. Then the following statements can be made [10],

$$\lambda_2 \leqslant vc \qquad \lambda_2 \leqslant ec$$

To the eigenratio λ_2 / λ_N, by the previous relations the following upper bounds can be stated,

$$\frac{\lambda_2}{\lambda_N} \leqslant \frac{k_{min}}{k_{max}} \leqslant 2\frac{m}{n}$$

Because row sum of L being equal to 0, the following equation can be built up.

$$\boldsymbol{L}\cdot\vec{1}=0\cdot\vec{1}$$

L is a singular matrix with the 0 eigenvalue and the [111..] eigenvector.
Generally the eigen-equation,

$$\boldsymbol{L}\cdot\vec{v}=\lambda_i\cdot\vec{v}^i$$

If there's a nonzero solution, then λ_i is the ith eigenvalue, and v^i is the corresponding eigenvector of λ_i to **L**. The eigenvalues of the Laplacian matrix is the feature of the graph connectivity, the eigenvector tells about the partitioning of the graph [9]. With reorganizing the equation it is possible to solve it for λ_i.

$$\left(\boldsymbol{L}-\lambda_i\cdot\boldsymbol{I}\right)\cdot\vec{v}^i=0$$

than,

$$det\left(\boldsymbol{L}-\lambda_i\cdot\boldsymbol{I}\right)=0$$

where **I** is the identity matrix.
By solving the *characteristic polynomial*, this N-th order polynomial equation for λ will have n solution including the repetitive ones. If a solution λ_i occurs m times in the eigenvalue list, than the multiplicity of λ_i is m. As it was shown **L** has the eigenvalue 0 and the [111..] eigenvector. This is emerges from the structure of **L**, and is true for all Laplacians. If a real valued matrix have complex eigenvalues, than it is the complex conjugate is also an eigenvalue of the matrix and this is true to the eigenvectors as well.

Using the properties of the Laplacian and the Incidence matrix, some implications can be made about the graph. The eigen-equation can be written in the following form,

$$\boldsymbol{I}\cdot\boldsymbol{I}^{\boldsymbol{T}}\cdot\vec{v}=\lambda\cdot\vec{v}$$

multiplying it from the left with v^T, i.e. the transpose of v,

$$[\vec{v}^{\,T}\cdot\boldsymbol{I}]\cdot[\boldsymbol{I}^{\boldsymbol{T}}\cdot\vec{v}]=\lambda\cdot\vec{v}^{\,T}\cdot\vec{v}$$

by substituing $y=\mathbf{I}^T*v$,

$$\vec{y}^{\,T}\cdot\vec{y}=\lambda\cdot\vec{v}^{\,T}\cdot\vec{v}$$

and because the v^T*v dot product of a vector v gives the square of it is norm, λ can be expressed in the following way,

$$\lambda_i=\frac{\left|\vec{y}_i\right|^2}{\left|\vec{v}_i\right|^2}$$

y has the dimension of |E|=m, and

$$\boldsymbol{I}^{\,T}\cdot\vec{v}_{\,e=ij}=\vec{v}(i)-\vec{v}(j)$$

than λ can be written as

$$\lambda=\frac{\sum_{e=1}^{M}\left(\vec{v}(i)-\vec{v}(j)\right)^2}{\sum_{i=1}^{N}\vec{v}(i)^2}$$

Because λ is produced by the division of two non-negative number, it is always non-negative, thus **L** is positive semi-definit matrix. Also the 0 solution at v(i)=v(j) for every i->j edge can be seen. This also explains why the multiplicity of 0 in the eigenvalues gives the number of connected components. Nodes, which are reachable to each other had to have v values equal, we get a plus degree of freedom in choosing v with every plus independent connected component.

Network Dynamics

The dynamics of the signal flow are the characteristics of the network function with the constrain of the network structure. Signal transfer between nodes happening trough the paths, but to take account all the possible path between all pairs of nodes, would require high computational times, so for efficient working only the shortest paths could be assumed to take relevant part in the signal processing.

Synchrony

Synchrony is the feature of a system dynamics, described by equality of state variables in the course of time. First, synchronization in periodic system was investigated, like hanging pendulum clocks synchronizing their oscillating phase, but recently chaotic systems got more attention with their possibility of different kind of oscillations.

Several types of synchronization regimes can be determined, e.g. complete and general synchronization assumes identical elements activating together, or together in connected subsystems. Although, non-identical oscillating elements can reach phase-synchronization with differing amplitudes, but with the same phase of activation. If the oscillations are not in the same phase, but still has the same periodic time, than it is a phase-lag synchronization, with a constant difference lag time τ in the phase. In a chaotic dynamical system this regimes can combine specially where information needs to be stored and processed, like in the brain.

Master stability approach, [9] is used to model the system of coupled oscillators, and have the form,

$$^{i}\dot{x} = F(^{i}x) - \sigma \sum_{j=1}^{N} L_{ij} H(^{j}x)$$

where ^{i}x is the state variable of the node i, F is the internal dynamics function, H is the coupling function, σ is the coupling strength, and L resembles the Laplacian matrix of the network.

For small coupling strength the oscillators work on their own frequencies, for high values with the strong connections the nodes can synchronize more. Theres a threshold from incoherency to synchronization at the critical coupling strength σ_c

The Kuramato order parameter, |z|, can be used to measure the synchrony of the system by it is current state, not the structural organization. it is small close to the asynchronous state and also if it is balanced with synchronous subsystems in opposing state.

$$z = \frac{1}{N} \sum_{j=1}^{N} \mathrm{e}^{i x_j}$$

Constituting the current state with the deviation from a particular synchronous state $x_i = \delta x_i + x^*$,

identical nodes and so invariant x* is assumed, than the above equation can be written in the form,

$$\dot{\boldsymbol{\delta X}} = [\mathbf{1}_N \times \boldsymbol{JF} - \sigma \boldsymbol{L} \times \boldsymbol{JH}]\boldsymbol{\delta X} \qquad \boldsymbol{\delta X} = \sum_{i=1}^{N} \vec{v}_i \times \xi_i(t)$$

where J is the Jacobian operator, and v_i is the transverse eigenvector of the symmetric L. With applying v^T_j from the left side,

$$\dot{\delta\xi}_j = [JF(x^*) - \sigma \lambda_j JH(x^*)]\delta\xi_k$$

where, λ_k is the eigenvalues of **L**.
To investigate the effects of the structure, **L**, the Lyapunov exponents of the above differential equation have to be searched, in the function of the eigenvalues and the coupling strength $\Lambda(\sigma\lambda)$. It determines how fast the system reaches the x* synchronized state. The largest exponent is called the master stability function. A system to reach a stable synchronized state is accounted λ_N/λ_2 to be small [9].

Synchronizability

Upon the structural foundation of convergence and divergence, synchronizability also determined by neurophysiological factors. Synchronizability, the stability of a synchronized state. Maximal in unweighted fully random networks with uniform degree distribution. By optimizing with wiring length an optimal synchronizable network falls into the small-world regime [7].
In a computational model of phase synchronization between coupled neurons the balance between high clustering and short average path length, properties associated with small-world characteristics influenced the proportion of local to global synchronizations [14].

The largest absolute eigenvalue of a matrix is called the *spectral radius, ρ.* For the Laplacian it is inversely proportional to the critical coupling strength $\sigma_c \sim 1/\lambda_{max}$ [7]. The higher the maximal eigenvalue, the smaller σ_c, thus the network can reach the synchronization regime easier.

The more spread out the eigenvalues of L, the more likely the synchronous state will be unstable [9]. By the eigenvalues of symmetric Laplacians, a measure for the spreadness of the eigenvalues can be estimated by the ratio of the largest and smallest non-zero eigenvalues, the closer it is getting to 1, the more stable the synchronous state in the system [9].

II.3. The role of targeted attacks in studying networks

Robustness and vulnerability

By deleting edges or nodes from anatomical and functional networks with random deletions or with targeted attacks different vulnerabilities of the network can be determined. Inspecting the malfunctioning of networks while removing of it's elements has an important practical use. Many natural networks have to keep up it's function in a noisy environment, where nodes and edges can be easily failed. Nodes and edges for which removing the network function sensitive to can have and important role, and identifying these elements are important in understanding the network operation. A deletion is called an attack if it's targeted to a particular class of network elements.

These elements can be a class of nodes or edges determined by the aid of network analyses, e.g. shortest paths encode information about the network structure, constructing global centrality measures based on shortest path properties then identifying vulnerable edges and nodes is a method can be used to begin the robustness analyses.

Different measures of robustness can be originated depending on weather it is referred to the changes in structural integrity after edge or node deletion, or to the effects of perturbation on network states [14]. Vulnerability of a network can be studied by investigating some quantities at each deleting step. These vulnerability characterizing quantity changes include average shortest paths or diameter to increase faster, or decreasing transiency related to decreasing clustering coefficient. Or change of dynamical properties as less synchronizability are a way of vulnerability characterization. Resilient networks show less change in these quantities after deletion.

Static tolerance of the network refers to the robustness without the need of redistributing quantities, while in dynamical robustness the dynamics of redistribution of flows are taken into account [9]. Robustness can be analyzed with percolation theory, since the connectedness of the network to a giant component is marker of functional network communication [9].

Some network quantities followed during the elimination can be related, as the average geodesic have a natural connection with the diameter and statements can be made about the connected components e.g. during edge elimination a directed graph first will loose it is strongly connectedness, then at a later elimination the weakly. Also relation between the algebraic connectivity and the nr. of connected components are assumed. The algebraic connectivity is a good measure of vulnerability of undirected graphs because it is magnitude indicates connectedness. If λ_2 small, less edges are needed to remove to disconnect the graph. If it is 0 the graph is disconnected. Though it is proven for undirected graphs, the relation of undirected λ_2 and connectivity is not well known. Assumptions can be made with reconciling the nr. of connected components with the real part of the directed λ_2.

Different network topologies show different attack vulnerabilities and natural adaptive networks should possess special robustness to these sensitive targets, e.g. scale-free networks show resilience to random targeting, but tend to be vulnerable to targeting of high degree nodes, while brain functional networks lacking the high degree nodes with the exponentially truncated power law degree distribution, thus they are less vulnerable to high degree targeting [14]. Also the cortex was shown to be resilient against random attack [14], robust to random edge removal [11].

Node elimination is a widespread method to investigate neural network functions, e.g. cortical hierarchies, in [18] driving function of the pathways were tested and feed-back connections were identified.

Goals

Network properties and their use as Vulnerability Measures

Network properties as the degree distribution, *ASP,* the *diameter* and the *Clustering Coefficien*t together with the eignevalues of the Laplacian is by itself interesting to analyze, how the quantities retrieved from the cortical network of the macaque preserve after randomizing the network. With the two types of randomizing, one with rewiring the connection but keeping the original degree distribution, and another with Erdős-Rényi type random networks with same nr. of nodes and edges allows to examine how the quantities relate to the degree distribution of the network.

The changes in the important network quantities such as the ASP, diam, and CC to removing edges from a graph will describe its vulnerability to the remove bias and it's a good matter of question which quantity change describes well the network vulnerability.

Centralities

A question also examined is how different centrality measures relate in effects of vulnerability. Centrality measures like *EB*, *CD* and *Overlapping* was introduced here, a question is what are the sensitive centrality measures, i.e. attack strategies to certain vulnerability measures, and also in what extent the effect of the centrality measures resembles each other.

Topologies

Different centrality measure as an attack strategy can have different effect on the network depending on the topology of the network. To unfold the impact of the special degree distribution of the cortical organization on the different resilience attributes we compare its robustness to a similar ER random graph.

Also the certain vulnerability measures the graphs sensitive or resilient to can describe the network topology so it is a matter of question we investigate.

The question of the effects of the disturbance in the cortical hierarchy is examined by removing selectively convergent and divergent edges of the signal propagation, expressed by the CD for each edge of the network.

By the three type of network analyzed here we raise the question how a random network with a special degree distribution relate to the well known Erdős-Rényi random graph and then how the natural network of the large scale representation of the macaque cortex being one instance of that special set of degree sequence relate to its randomized version.

Robustness

Robustness can be derived form the vulnerability measures stated above, but an obvious degree of vulnerability is when a network separates, thus falls to disconnected components. Thus, robustness will be studied here by analyzing the nr. of connected components, moreover working with directed networks, the nr. of strongly connected components and the nr. of weakly connected components as the measure of robustness will be analyzed separately.

The relation between the algebraic connectivity, i.e. the second smallest eigenvalue of the Laplacian, and robustness is known and discussed in the introduction, thus algebraic connectivity could be a good measure of robustness to analyze. Although, it should be noticed, that in directed graphs the eigenvalues are more complex and less understood. To understand more the relation between the real part of the directed algebraic connectivity and connectedness, the changes of the algebraic connectivity and the nr. of connected components will be analyzed collectively.

Synchronizability

As it was shown, synchronizability of a network can be resembled to the spreadedness of the eigenvalues of the Laplacian, represented by the *eigenratio*. Thus, here to understand the vulnerability of the synchronizability, a function well needed to cortical processing, we investigate the changes in the *eigenratio* to removing certain class of edges, with a special interest to convergent/divergent edges which are known to play role in synchronization.

Methods

In this works generally graphs without self-loops were used. The macaque visuo-tactile cortical network were analyzed, consisting of 44 nodes and 630 directed edges. The underlying adjacency matrix representation was based on unweighted connectivity data published originally in tract-tracing studies [6]. In addition 30-30 instances of randomized networks with and without conserving the cortical degree distributions is used for comparison, average values are plotted with deviation.

For the illustrations, simulations and computations the GNUplot, Octave and the R environment was used with the addition of the free igraph package [http://igraph.org/r/] for graph generations, randomizations and shortest path calculations.

If a graph is not strongly connected, there's at least one pair of nodes where there's no path between, so we have to decide how to interpret shortest path in the computation. Igraph offers two methods, with method A we only consider the existing paths in the average, with method B we assign to the nonexistent paths the number of vertices in the graph, which is one greater than the longest path possible in the graph.

Two types of random graphs were used in this work, both with the aid of the R igraph package . The rewired random graph were used with the rewire function of the package [http://cneurocvs.rmki.kfki.hu/igraph/doc/R/rewire.html] with preserving the degree distribution of the original, cortical, graph. The number of iteration of the rewiring were 10 time the nr. of edges in the graph. For the Erdős-Rényi random graph igraph offers a function of network generation [http://igraph.org/r/doc/erdos.renyi.game.html] called erdos.renyi.game, and the “gnm” type were used, with the parameters, node nr. n=44 and edge number m=630, resembeling the original cortical graph.

Here when giving the clustering coefficient directed graphs are considered as undirected, this means all topologically different triangle motifs considered, the 111, 11-1, 110, -110, 1-10, 001 000, where the minus means the other direction in the cycle, 0s are the reciprocal connections. Also, given a node with k neighbors, the number of possible links in the neighborhood is $k(k-1)$. Note that this would result in a division by zero if $\underline{k} = 1$ (i.e., if the node has only one neighbor), hence we excluded all the vertices with degree less than two from the clustering coeffitcient calculations.

Edge deletion

In this work the method of understanding the importance of edge properties in the function of the network is trough characterizing its vulnerability with targeted and random edge removal. The edges selected to remove by their assigned measures based on their shortest path properties. Edges with the highest values of the following quantities were removed,

- Edge Betweenness (i.)
- Convergence Degree (ii.)
    - absolute value (a)
    - maximum value (b)
    - minimum value (c)
- Overlapping Set (iii.)

And to compare network vulnerability with edges chosen without any bias, in each case we performed an attack with randomly picked edges too (iv.).

It is important to decide whether to quantify the edge properties in each iteration or to use the ones calculated from the initial network. Recomputing was chosen, as removal of the edges alter structure, important edges by the initial computing can loose significance, and the attack strategy

looses to pronounce vulnerability [1]. Also brain plasticity after lesions suggest the adaptation of functioning to the small changes in the structure, therefore the importance of the connections should be determined by the actual network structure.

Then to determine the attack damage and reorganization of the cortical network, changes were compared by means of computing various network properties, as average shortest path, diameter, clustering coefficient, the number of strongly/ weakly connected components, the second smallest/largest eigenvalues of the Laplacian matrix, to reveal the changes in the global signal propagating properties the changes in the convergence degree sum were illustrated.

The independence of variables (x) of the control networks (the rewired and ER) were tested with independent t-test in the following form,

$$t = \frac{\bar{x}_{ER} - \bar{x}_{rew}}{\sqrt{\frac{s_{ER}^2 - s_{rew}^2}{N_{sample}}}}$$

where in the nominator the differences of the mean sample variables, s is the standard error of the sample and N is the sample size = 30 in our case.
If the calculated t value is larger than the critical t value the independence probably hold true with p=1-α (α see below).
With the degrees of freedom (the sum of the two sample size minus two, df=58) and the alpha level (α) the critical t value can be identified from the t table. With α=0.05 the critical t value is 2 and it stays below 2.7 at α=0.001.

Results and Discussion

Comparison of the cortical and random networks, network properties and their use as vulnerability measures

Data are summarized in [Table 1- 3.].

Table 1.

	density	diam	asp	clustering coeff
cortical	0.33	3	1.775	0.616
rewire	0.33	3.27 +- 0.45	1.712 +- 0.009	0.616 +- 0.009
ER	0.33	3 +- 0	1.671 +- 0.002	0.554 +- 0.009

Table 2.

	λ2	λmax	λ2/λmax	cdsum
cortical	2.84	30.0796	0.0944	-24.4
rewire	4.05 +- 0.05	29.77 +- 0.11	0.136 +- 0.002	-30.5 +- 3.09
ER	8.27 +- 1.28	21.64 +- 1.26	0.383 +- 0.065	-0.008 +- 3.633

Table 3.

	inital extreme edge values				
	EB	Cdabs	Cdmax	Cdmin	Ovl
cortical	43.01 +-	0.95	0.95	-0.94	0.26
rewire	46.6 +- 10.1	0.94 +- 0.01	0.93 +- 0.01	-0.93 +- 0.01	0.36 +- 0.05
ER	10.9 +- 1.3	0.65 +- 0.07	0.61 +- 0.07	0.61 +- 0.06	0.39 +- 0.04

All the random variables after the t-test were found to be independent, i.e. at p=0.05 significance the control random network measures examined were found to be distinct, had a higher t value, than t_c =2 [Table 4- 5.].

Table 4.

variable	t values
diameter	3.3
asp (agp)	25.6
cc (clustering)	82.4
λ2	18.1
λmax	35.5
λ2/λmax	20.8
cdsum	87.4

Table 5.

	variable	t values
inital extreme	EB	19.5
	Cdabs	22.9
	Cdmax	25.3
	Cdmin	19.6
	Ovl	5.5

The *reciprocity* of the macaque network was found to be 0.77, i.e. 77% of the connections were reciprocal. The number of nodes and edges was preserved in the random networks, so the density is. The *density* of the cortical network was higher than in [11] where it was found to be 0.16 of macaque networks with average shortest paths to be 2.2 and clustering coefficient to 0.46. To the higher density smaller average shortest path and higher clustering is expected, and found here.

The *average shortest path length* were found to decrease after randomizing the cortical network, taking the smallest value for the ER, consistent with the known small *ASP* of ER random networks. The higher *ASP* in the natural network can be well related to the spatial constraint of such a networks.

The *diameter* was highest in the rewired network, smaller in the ER. Interestingly in the cortical network was smaller than in the rewired, despite the ASP showing different relation. Though, the differences are not prominent.

The c*lustering coefficient* was higher in the rewired network than in the ER. In the cortical was found to be identical as in its rewired version. For both randomized networks, the deviation was very small. The to three decimal places identical *CC* of the cortical and rewired networks can hold in the preserved degree distribution and in the preserved *density*, but as the density was the same in the ER as well, the relation could be in the special degree distribution.

The cortical network had a heterogeneous *degree distribution* [Fig. 1.]. The distribution represented here contains both the in and out degrees, thus the maximal possible degree is (N-1)*2=86. In the macaque the maximal degree k_{max} =59, while k_{min}=8.

With the maximal and minimal degrees its possible to estimate the eigenvalues of the undirected Laplacian of the cortical network. The estimation gave $\lambda_2 < 8.19 < 29.3$ and $60,37 < \lambda_{max} < 118$ and $\lambda_2/\lambda_{max} < 0.13 < 28.64$. These estimations are partly fitting with the results, being valid to the second smallest eigenvalue

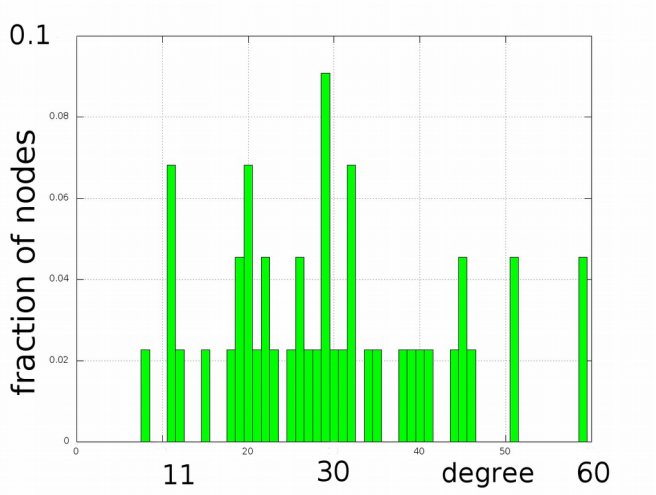

Figure 1. *Degree distribution of the cortical network*

and the eigenratio, showing the difficulties of identifying the directed eigenvalues.

The *highest EB* was significantly smaller in the ER random than in the rewired cortical, as usually expected to have more homogeneously distributed edge properties in the ER graphs. The cortical network was fallen into the rewired regime. Similar results were found to the *CD values*. The diverse degree distribution can explain the larger EB and CD values in the cortical and rewired cortical networks.

Through the 1-|CD|<Ovl relationship, the lower limit in the rewired is decreasing compared to ER, which was seen as the maximal *Overlapping* values were smaller. In the cortical network the maximal Overlapping was prominently smaller than for the random networks.

As expected due to symmetry of the edge generation to the directions the *CD sum* of all edges was nearly zero for the ER network. Oppose to that the cortical networks were significantly asymmetrical with negative CD sum. The high negative CD sum in the cortical network could mean higher amount of divergent connections, and/or could mean more divergent connections. During the CD minimal and maximal target deletion [Fig. 4-5] the edges got removed had similar magnitude in minimal and maximal CD values, only showed difference at the placing of the marked behaviors in the removing process, indicating the assumption of having the asymmetry in the higher nr. of divergent edges, then having similar distribution of convergent/divergent edges in number, but them being overall more divergent. In the macaque network the CD sum was lower negative value then that was seen in the rewired network.

The *algebraic connectivity* of the ER graphs was twice than that of the rewired random graph, and the cortical network had the smallest value, half of the rewired. The deviation of the eigenvalues [Table 2] being at least one order smaller to the rewired networks with fixed degrees shows how the fixed degree sequence puts a large constraint on the eigenvalues, thus the connectedness.

The λ_{max} associated with the ER graph was the smallest, and λ_{max} was slightly higher in the cortical than in the rewired networks. The maximal eigenvalues also showed the decrease in the deviation in the rewired compared to the ER network.

The ratio of eigenvalues λ_{max}/λ_2 was the closest to 1 in ER, the rewired had less than that and the cortical got the smallest value. Thus indicating the strongest synchronizability for the ER, and the least synchronizability as indicated by the ratio was exhibited by the cortical network.

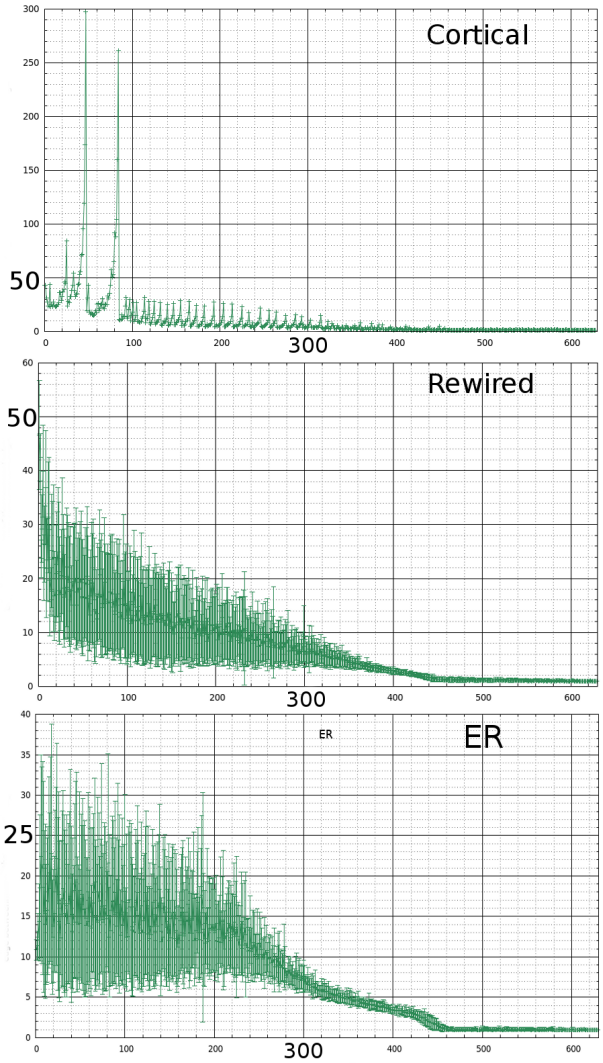

Figure 2. *EB of the edge removed in the function of the nr. of edges removed (at EB target)*

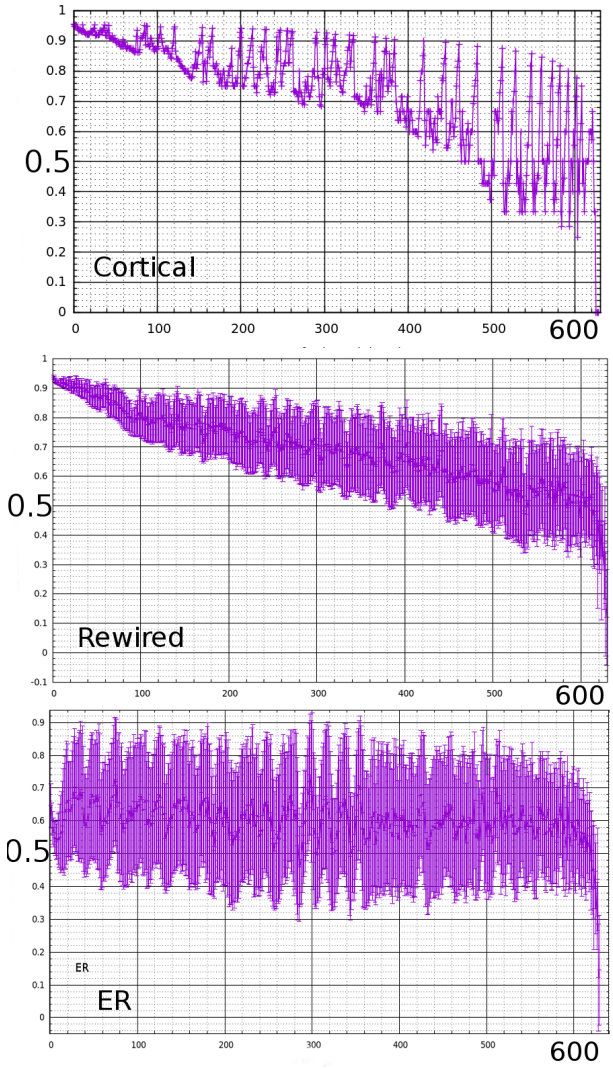

Figure 3. *Absolute CD of the edge removed in the function of the nr. of edges removed (at CD abs target)*

The inhomogeneous structure, i.e. higher extreme edge values, the well clustered form and the small λ_2 of the macaque network indicate less well connected structure, which is easier to disconnect than a random network, and while it is seem to be contrary with the needs of a resilient brain network, the restriction of the physical embeddedness can make this property understood. Diverse CD values allow a more complex information processing, beneficial for the complex brain function.

As the measure of complete synchronizability, the eigenratios indicate that the randomized networks, specially the ER networks is the easiest to synchronize. This confirms the inverse relation between synchronizability and the heterogeneity of a degree distribution [21]. These synchronizability properties are denote complete synchronization, which is in a healthy bran is a pathological form and only can be seen during epilepsy [8]. Thus the brain structure rather should avoid this regime and should be able to maintain a less complete, more complex synchronization manifold with easily changing states while performing different cognitive functions.

Targeted edge removing

While for the ER networks most of the properties showed symmetrical change in minimal and maximal CD based removing, the networks with the cortical degree distribution was asymmetric in

the convergent and divergent edge remove.

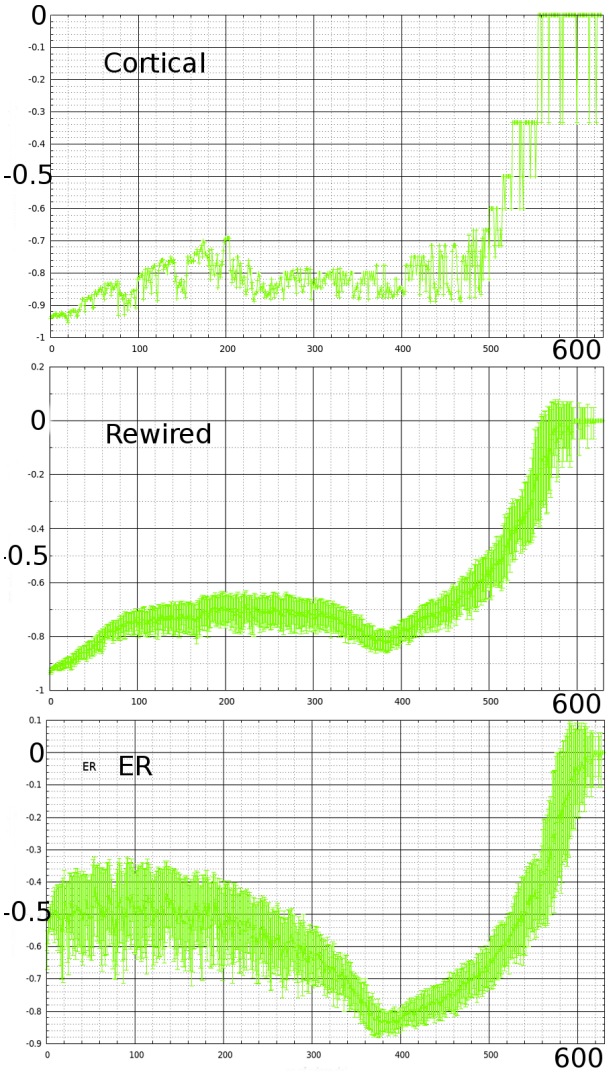

Figure 4. *The CD of the edge removed in the function of the nr. of edges removed at minimal CD target*

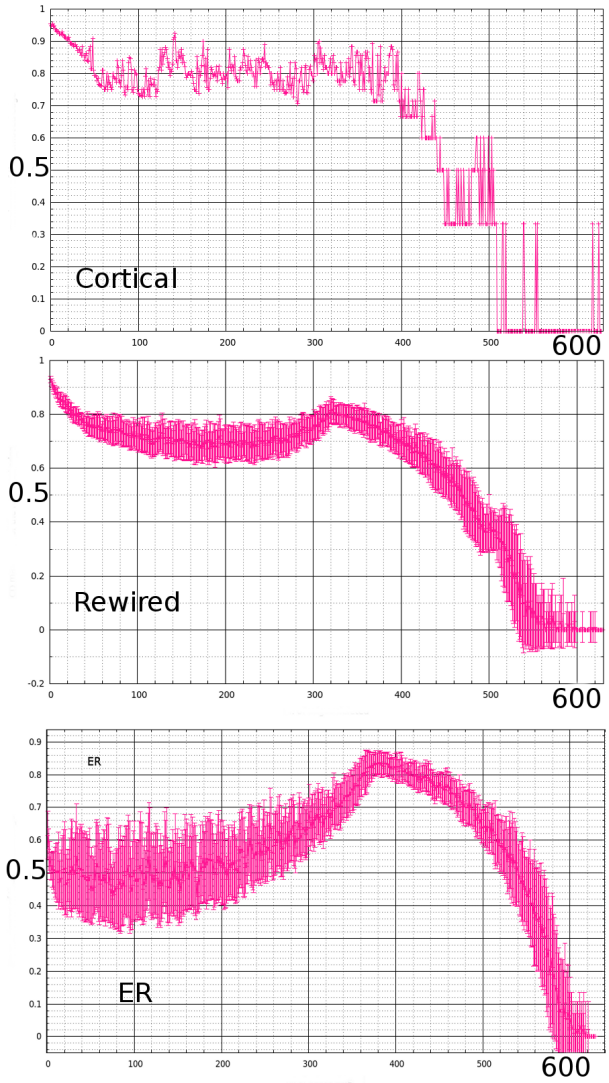

Figure 5. *CD of the edge removed in the function of the nr. of edges removed at minimal CD target*

Extreme edge values, i.e. values of the edges removed

In the ER networks the EB and CD abs values of the removed edges are smaller than in the networks with cortical degree distributions [Fig. 1-2.]. *Edge Betweenness* values in the cortical network resembles to the rewired with occasional peaks of high valued edges.

CD absolute values in the ER were more homogeneous and smaller as in the rewired networks. CDs in the rewired were close to the maximal value 1 with small deviation [Table 3.], and as the less edge stays in the rewired graph the CD decrease and its the deviation increase, while in the ER it stays consistent through the whole process [Figure 3.]. The cortical network had a very similar form in the CD absolute values as the rewired.

The high deviations are due to the change of the maximal CD absolute during the separation of the graph. The peaks in the maximal CD abs., what's present in the individual case of the cortical network, are corresponding to the disconnection of the network. The CD abs increase to the peak and falls after the separation of the network. The peaks averaged on several networks can result the

large deviation.

The rewired network had slightly higher means of *Overlapping* than the ER and showed higher deviation, which was increasing as the more edges got removed. The cortical Overlapping values were prominently smaller with peaks of high valued edges.

After removing more than half of the edges with the highest Overlapping Set, 51.7% from the rewired and 53% from the ER, will result in a drop to zero Ovl values, meaning the lack of chordless cycles in the network after that point [Fig. 6.]. The change in the highest overlapping set shows very similar form in the ER graph and in the rewired, just the ER shows higher mean at the first steady part before the sudden decrease. Although, the cortical network values were smaller, almost the half of the rewired with averaging it can fit to the rewired regime. Though, the cortical seem to reach the overlapping set free state sooner, after 40.6% of the edges removed.

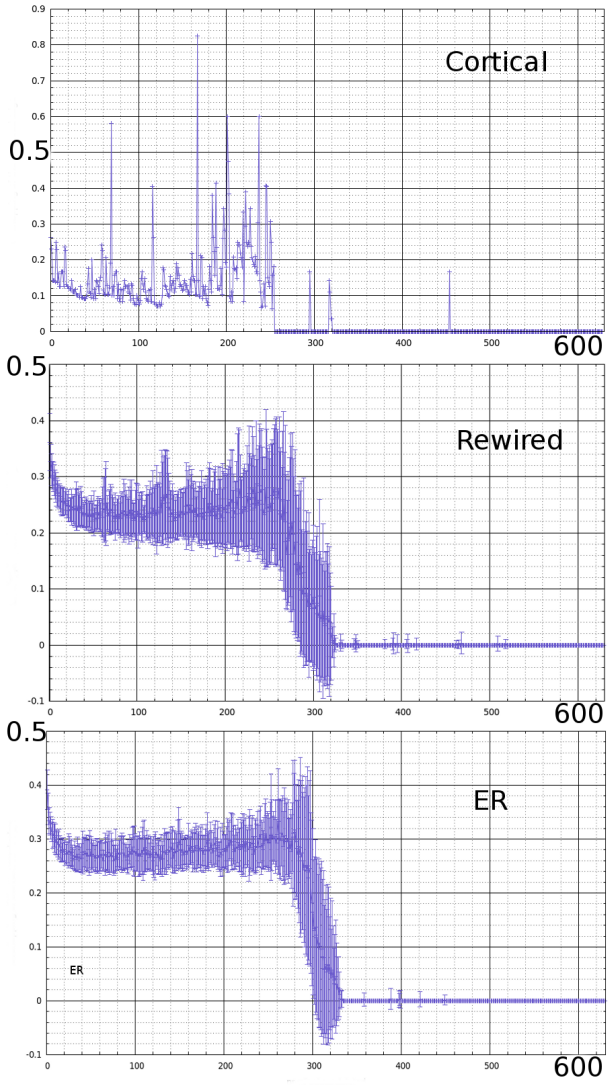

Figure 6. *Overlapping of the edge removed in the function of the edges removed at highest overlapping target*

The absolute CD values of the edges removed at the *maximal CD and minimal CD* target are smaller in the ER and than in the rewired [Fig. 4 and Fig. 5], and the cortical network resembles the rewired.

In the signed CD values a local minimum and maximum can be seen in the function curve. Thought, the ER is symmetric in the amplitude of the values and in the place of the local extremes, in the rewired graphs an asymmetry in the place of the extremes can be seen, as at convergent (CD max) target it reaches it approx. 60 edge removing (~10% of the all edges) earlier.

From the higher CD and EB values of the edges deleted, the cortical and its rewired networks are not only more heterogeneous in the node degrees, but in the convergence degree of the edges as well. Combined with smaller Overlapping in the cortical and in the rewired a more directed information processing can be assumed, than what is present in the ER networks. This is supporting the cortical network to be more hierarchical with the aid of the degree distribution.

Vulnerability by the average shortest path length

To the ASP vulnerability measure EB was the mast effective target, while to random and Overlapping based attack showed high resilience in all 3 types of networks. Convergence Degree based targets had similar effect to each other and was

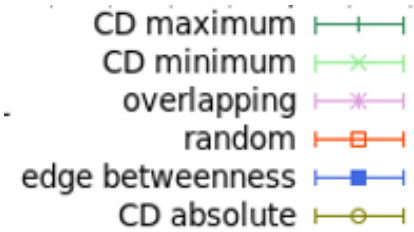

Key 1. *Color code for target measures used and illustrated together in the following chapters*

an effective target to decrease ASP, but was not as strong as to EB.

The rewired compared to the ER network seemed to be more sensitive to the EB and CD based targets. Asymmetry in the ASP vulnerability was present at the rewired network and was more sensitive to the convergent edge target.

By analyzing the cortical network during edge remove individual characteristics can be seen, e.g. the *ASP* in the cortical network in both method used at some steps the functions changes fast [Fig. 7. and Fig. 8]. This can be seen as a toothed structure with method A, and staged layout with B both caused by a connected component loosing it is connectivity at a specific edge, strong or weak. When this specific edge is deleted a set of nodes becomes unable to reach another, so all those path existing before the deletion connecting distant nodes with method A becomes excluded from the

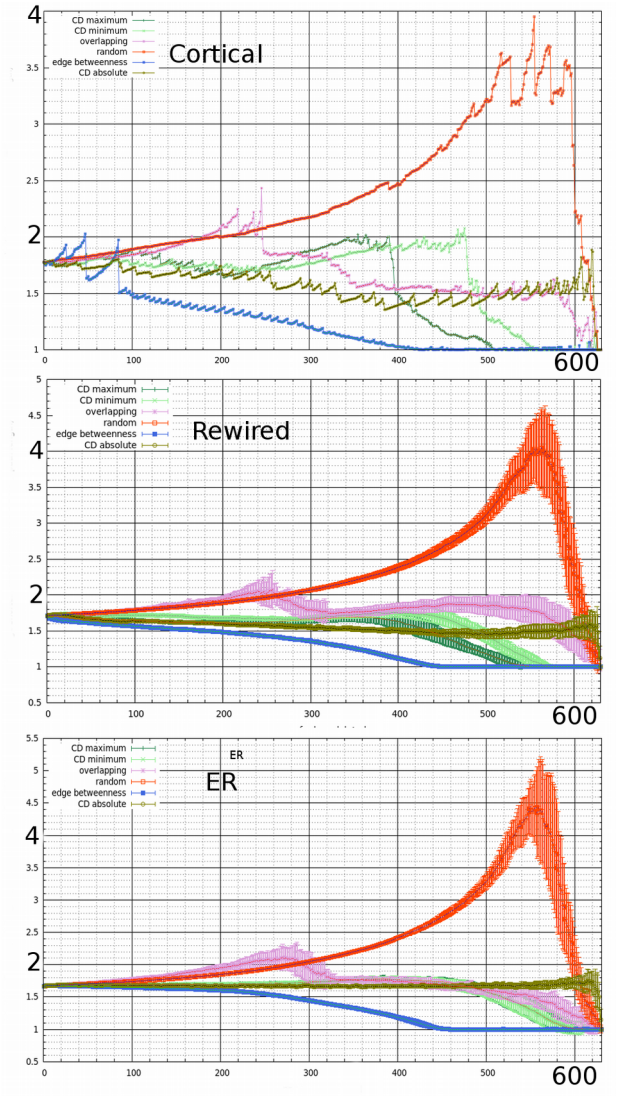

Figure 7. *Changes of the ASP (method A) in the function of the nr. of edges removed at different targets [Key. 1.]*

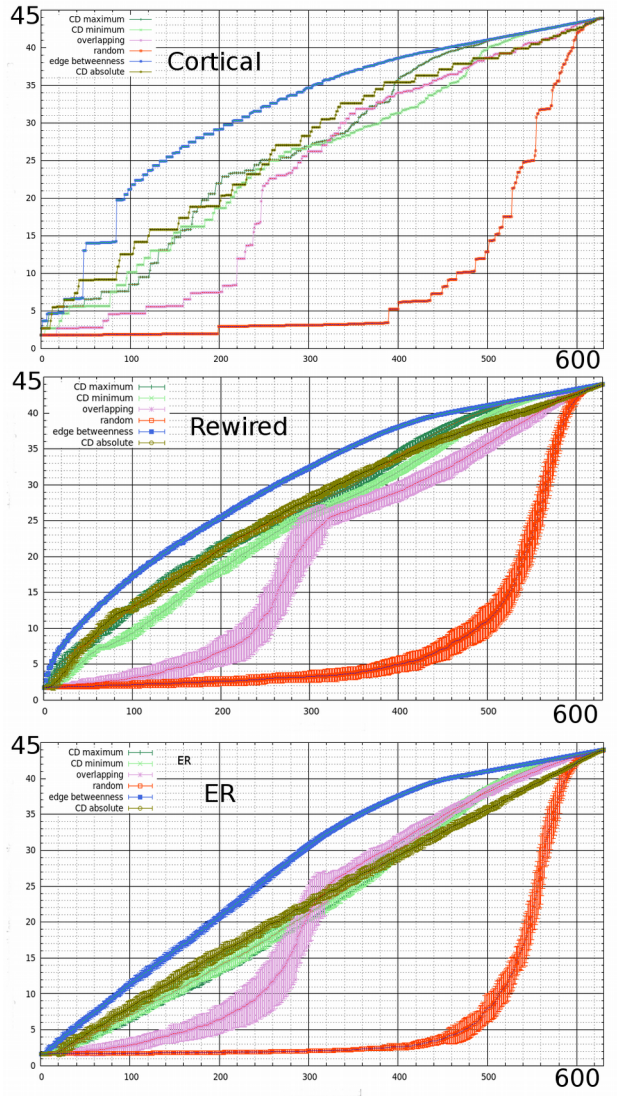

Figure 8. *Changes of the ASP (method B) in the function of the nr. of edges removed at different targets [Key. 1.]*

average, the *ASP* drops. Then the slow increase continues with the edge deletions until another specific edge is found. With B method the structure becomes staged, with the specific parts identical to the ones in method A. It is because the paths that gets excluded from the average in case A increases the asp with |V| at method B, |V| is the maximal path length possible plus one. Than it is clear that all the simulations with method B converges to 45, and to 0 at A. With method B the

increase is continuous, the surface under the curve proportional to the damage, what the edge removal cause with the specific target.

The most effective target being the edge betweenness, is understandable, because, the higher the edge betweenness, the more shortest paths goes through that edge, so by deleting it more shortest paths have to increase. *ASP* resilience to random edge remove was prominent compared to other targets. That is not a surprise, because all other measures depends on the shortest paths.

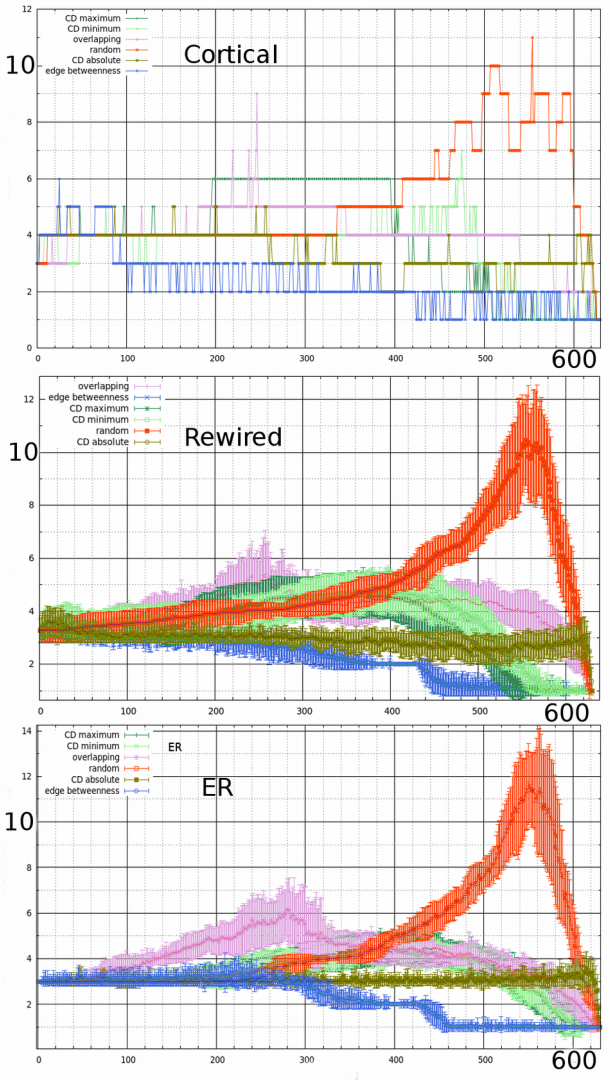

Figure 9. *The changing of the diameter in the function of the nr. of edges removed with different targets [Key 1.]*

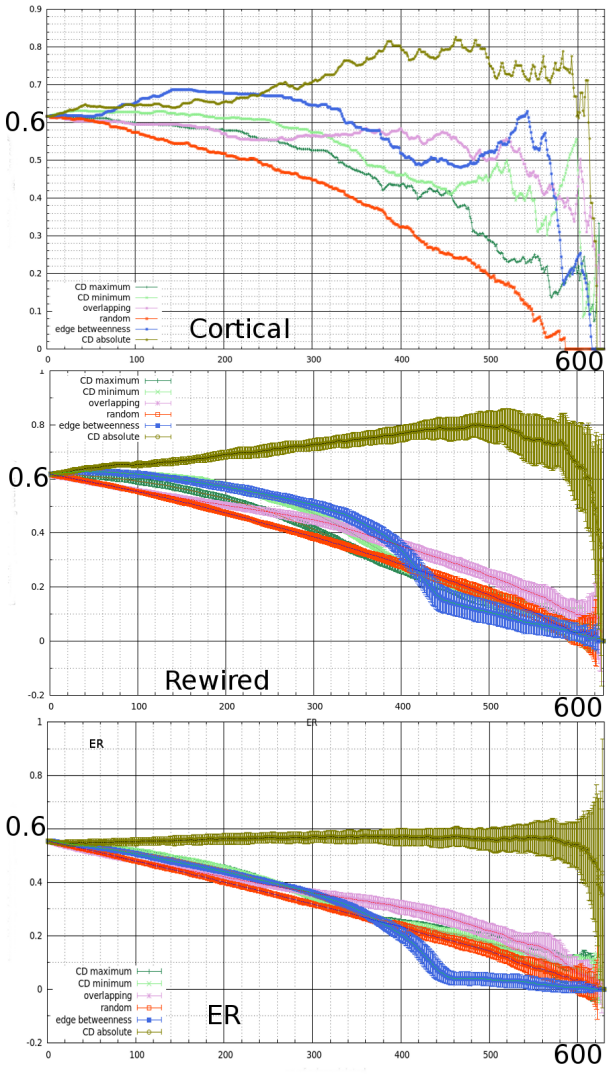

Figure 10. *The changes of the Clustering Coefficient in the function of the nr. of edges removed at different attack strategies [Key 1.]*

Similarity with the diameter

As predicted for the ER graphs *ASP ~ diam* can be seen on the similar figures of *ASP* method A and the *diameter* [Fig. 7. and Fig 9.]. This was present also at the rewired random networks. Interestingly, a region was present for both random networks where diam=2 with very small deviation was. Otherwise, similar consequences as from the analysis of the *ASP* can be made.

Clustering coefficient resilience

By the Overlapping and random target was the most effective to reduce CC in the networks [Fig. 10.]. Removing edges with the highest CD absolute had an outstanding effect with increasing CC. Edge betweenness and the signed CD targets showed similar results, but removing convergent edges from the rewired network had stronger effect then the EB target. In the rewired network more increase could be seen than in ER at CD absolute target. Interestingly, on the cortical network EB had stronger effect than after rewiring the network.

These effects can be the result of taking out Overlapping nodes when constructing the convergence degree. After 1>Ovl+|CD|, removing edges with high CD will leave edges with high Overlapping, which is proportional to the number of cycles containing an edge, including triangles, which determines the *CC*. Then, targeting edges based on their Overlapping expected to be an effective strategy to decrease the CC, but also bigger cycles can contribute to the Overlapping Set.

In the networks with cortical degree distributions at CD abs target the CC will increase to higher values. By the draw of the CD values of the removed edge [Fig. 3] it is known that from the rewired network higher CD absolute values were removed, which can be in relation with the higher increase of CC in [Fig. 10].

Table 6. *The nr. of the edges where the network strongly disconnects*

	Sconn=2	1.06<nr.of sconn comp<=2.06	
	cortical	rewired	ER
eb	2	2	6 – 13
cdabs	2 – 11	4 – 19	15 – 39
cdmax	2 – 8	2 – 7	11 – 30
cdmin	6 – 21	10 – 21	10 – 28
ovl	19 – 70	11 – 85	18 – 92
random	200 – 390	6 – 254	339 – 448

Table 7. *The nr. of the edge where the network weakly disconnects*

	Wconn=2	1.06<nr.of wconn comp<=2.06	
	cortical	rewired	ER
eb	107 – 429	10 – 28	440 – 461
cdabs	13 – 16	11 – 23	21 – 41
cdmax	501 – 504	485 – 535	434 – 492
cdmin	480 – 496	492 – 538	420 – 495
ovl	284 – 329	414 – 500	324 – 414
random	451 – 533	429 – 528	506 – 548

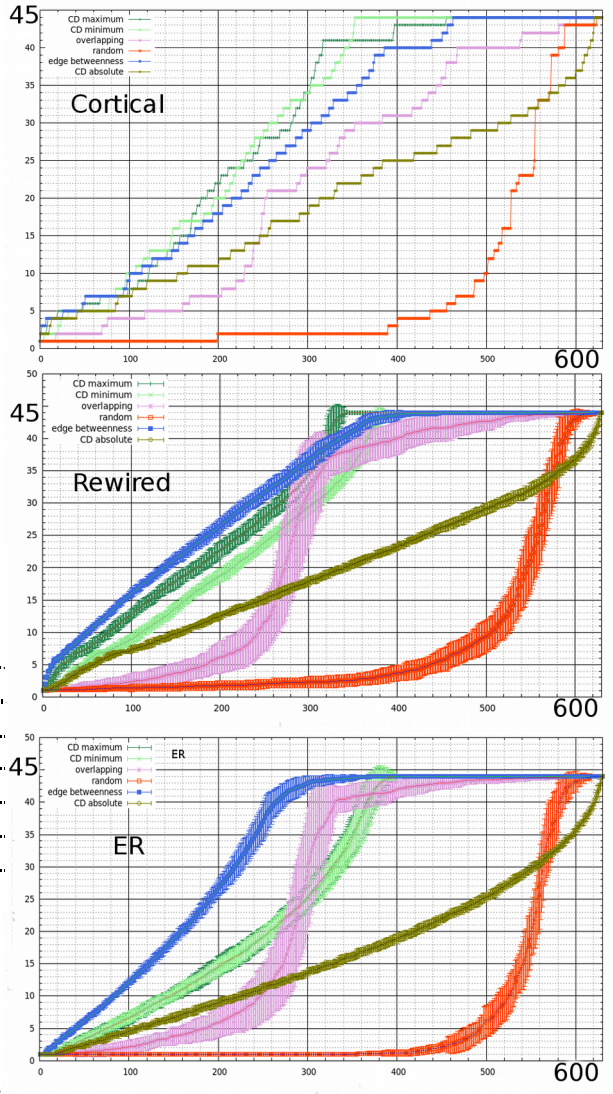

Figure 11. *The nr. of strongly connected components in the function of the nr. of edges removed at different attack strategies [Key 1.]*

The increasing number of connected components

Strongly connected

At the loosing of strong connectedness, the one way separation of the graph, the network were the most vulnerable to EB but showed high vulnerability to the signed CD based deletions as well, which were more efficient then the CD absolute target [Fig. 11.]. CD absolute target was in the middle in the strongness of the vulnerability range.

Interestingly, in the cortical network the signed CD deletions were the most vulnerable attack strategies to strong connectivity in the later parts of edge removes, while in the beginning it is not obvious, EB CD abs. Min. and max. had similar efficiency. The rewired network specially at the beginning of the attack process were more sensitive to EB and to CD derived quantities than the ER network. In the ER to the CD min and max targets the effects were symmetrical and had smaller steepness compared to the rewired networks, where the network was more vulnerable to the CD maximum based deletion. For random edge removing all networks showed high resilience.

EB target reaches the maximum strongly connected components in the ER network slightly sooner than in the rewire.

After removing edges with the highest Overlapping the network separates first slow and then very fast gets close to the maximal nr. of strongly connected components. When the network runs out of edges with non-empty Overlapping Set, the strong connectivity function converges slowly to the total separation, showing a phase-transition like behaviour.

If the graph contains clusters of vertices with increased amount of connections in the clusters, and a few connections between them, the shortest paths between the nodes in different clusters can go only through the few inter-cluster connection, which then will have increased edge betweenness, and gets deleted sooner, enhancing the clustering, then, the segregation of the network. This can reason the highest gradient of EB based removing on the nr. of strongly connected components.

A network having the maximal nr. of strongly connected components is lack of reciprocal connections, because the two node connected with the reciprocal connection are strongly connected.

When maximal strong connectivity is reached during edges removed by their signed CD, the signed CD values of the edge removed in the transforming network start to converge to zero [Fig. 4. and Fig. 5. Fig. 11].

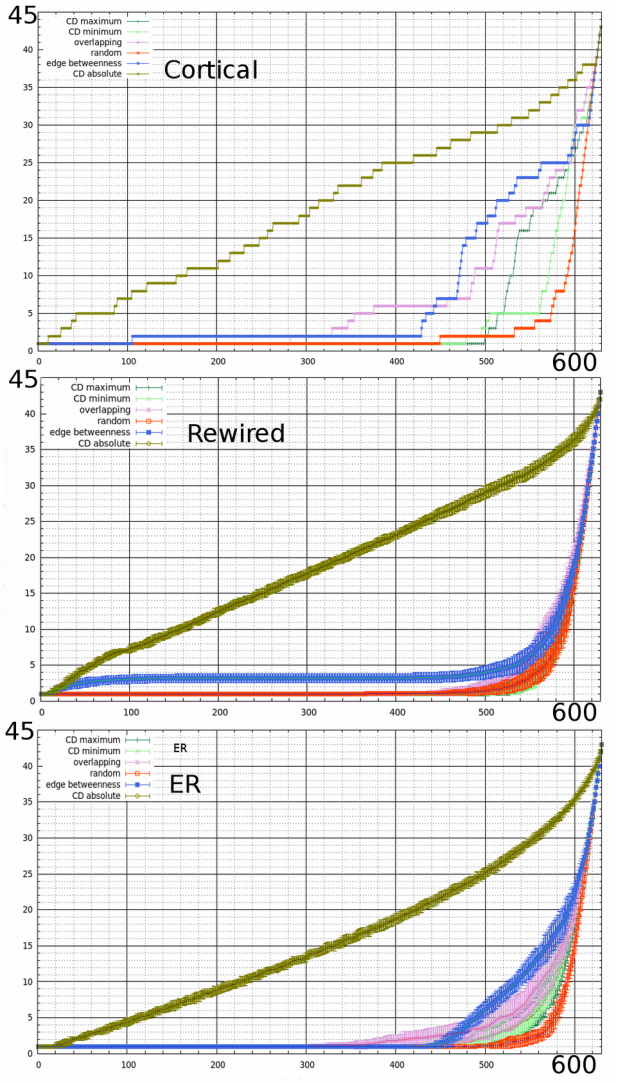

Figure 12. *The nr. of weakly connected components in the function of the nr. of edges removed at different attack strategies [Key 1.]*

The local extremes of the CD minimal and maximal values during the edge removes [Fig. 4-5] is at the point when the network reaches the maximal number of strongly connected components |V|, thus all pair of nodes can be connected only in one direction. This requires the absence of reciprocal and recurrent connections in the network.

At EB targeting the CC decrease with increasing gradient until the maximal EB gets close to 1 [Fig. 1.]. To this point the network also reached the maximal nr. of strongly connected components. Where the small CC possibly corresponds to the low proportion of (11-1) motifs. Other motifs are not allowed, because they have edges with EB>1 or contains reciprocal connections, which is not allowed, because then the nr. of strongly connected component would be <|V|.

Weakly connected

To loose the weak connectivity, so to result the network complete disconnection, absolute CD based removing was markedly the most effective [Fig. 12], and it had very similar results on strong and weak connectivity with similar gradient, which was slightly higher in the rwired than in the ER network. EB target did separated the rewired and cortical networks, but was not causing serious damage. All the other targets were separating the graph weakly at the end of the edge deletion.

In the rewired network to remove approx. 5% of the edges was enough to separate the graph to a few weakly connected components at absolute CD and EB target, but to further separations EB targeting was ineffective. The ER graphs did not disconnect until ~70% of the edges got removed with EB target. In the macaque network after removing 13 edge (2% of all) with the highest absolute CD the network separated to two unconnected components, while at EB target 107 edges (17%) were needed to be removed [Fig. 12.].

Independently from the type of network after 73% of the edges removed with EB based edge deletion, the maximal EB will not go much above the minimal 1 [Fig. 2.]. Before this point the nodes are still connected because the nr. of weakly connected components are small. With removing an edge the shortest paths that edge was part of had to go on another route and it will put a divided load on other edges, increasing their EB in the new structure. If the removed edge was a bottleneck in one direction, it will have a high EB value, and removing it will cause a drop in the maximal EB value. This process can be seen as the peaks in the macaque network are consistent with the strong (one directional) disconnecting.

EB, the signed CDs and the Overlapping first attack the strongly connectedness, while giving no effect on weakly connectedness. Only after getting close to the maximal nr. of strongly connected components will effect the weakly connectedness. Thus to total disconnect a directed network these measures are not efficient, while CD absolute is a good target to total disconnect the graph.

Changes in the convergence degree sum during elimination

Removing edges with the highest CD absolute, as expected, will result the CD sum fast convergence to zero, while with random targeting it converges slow [Fig. 13.]. Signed CD target increase the CD sum to the reverse sign, which is understood, removing convergent edges will make the network overall more divergent, and the other way with divergent edges. Interestingly, after reaching an extremum the CD sum changes sign fast and reaches another local extremum with the same sign as the target CD sign.

For the ER network minimal and maximal targeting had symmetrical results, while with the cortical degree distribution the inflexion point come earlier at convergent edge target, which supports the surmise of the higher number of divergent edges in the initial network.

Interestingly, at the rewired network the EB target got the CD sum more negative and reached zero later at the removing process, while in the ER no prominent results could be seen. During Overlapping based deletion ER graphs showed effects in the second phase towards a positive sum, although at that time only zero overlapping edges were removed.

The asymmetry in [Fig. 4-5] suggest the less convergent organization of the cortical degree distribution, and the CD sum being negative iof the rewired network seem to verify it.

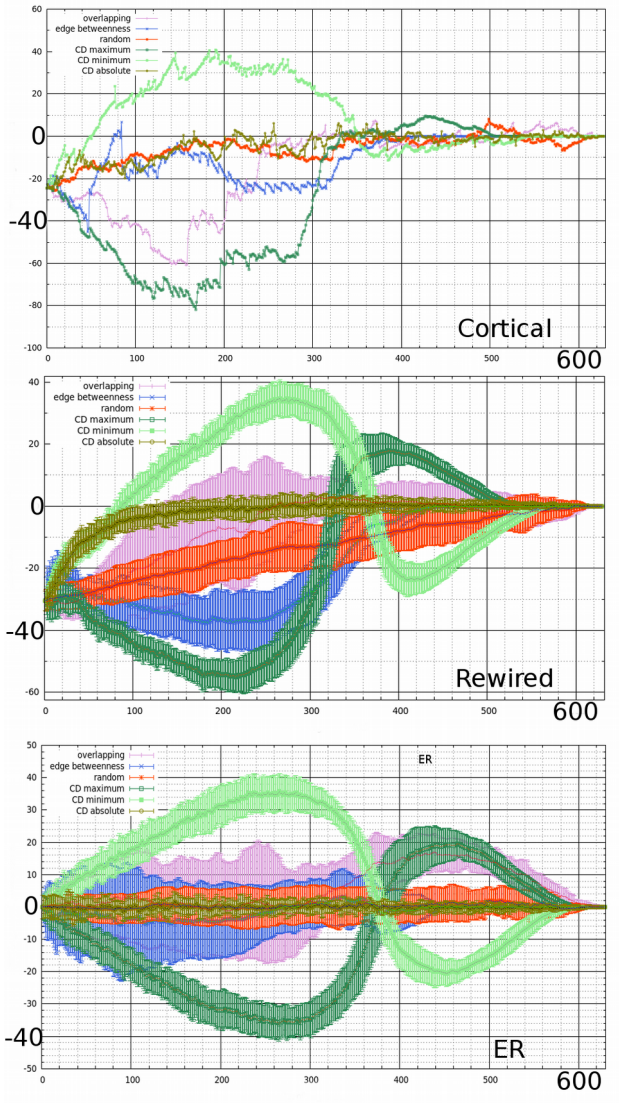

Figure 13. *Changes in the CD sum of the edges in the function of the nr. of edges removed at different attack strategies [Key 1.]*

***Spectral analyses during elimination**:*
CD as a sensitive measure of the robustness and dynamical properties of the cortical network

λ_2 vulnerability to the different targets

Sensitive targets to the algebraic connectivity were mainly the minimum CD, absolute CD and edge betweenness [Fig. 14]. Random edge elimination were somewhat featureless with converging to zero with a consistent small steepness. Overlapping showed behavior close to the random targets, but somewhat closer to the vulnerable targets. Eliminating edges of high positive CD, i.e. convergent edges, showed an interesting behavior with either giving increasing, or no or less effect than the random elimination.

In the ER random network the algebraic connectivity became 0 first with the absolute CD target, while in the rewired cortical random network CD absolute and minimal along with EB showed similar behavior in the vulnerability [Fig. 15.]. Interestingly the macaque network showed resilience to the EB based target [Fig. 14].

In the cortical network at almost all targets λ_2^{real} becomes zero less or more sooner than in its rewired network, and knowing the smaller initial λ_2^{real} it is can be explained. An interesting exception is the EB target, where λ_2^{real} decrease later (reach zero at removing 13.6% of edges) than as it is in the rewired networks (at 4.8%) [Fig. 15].

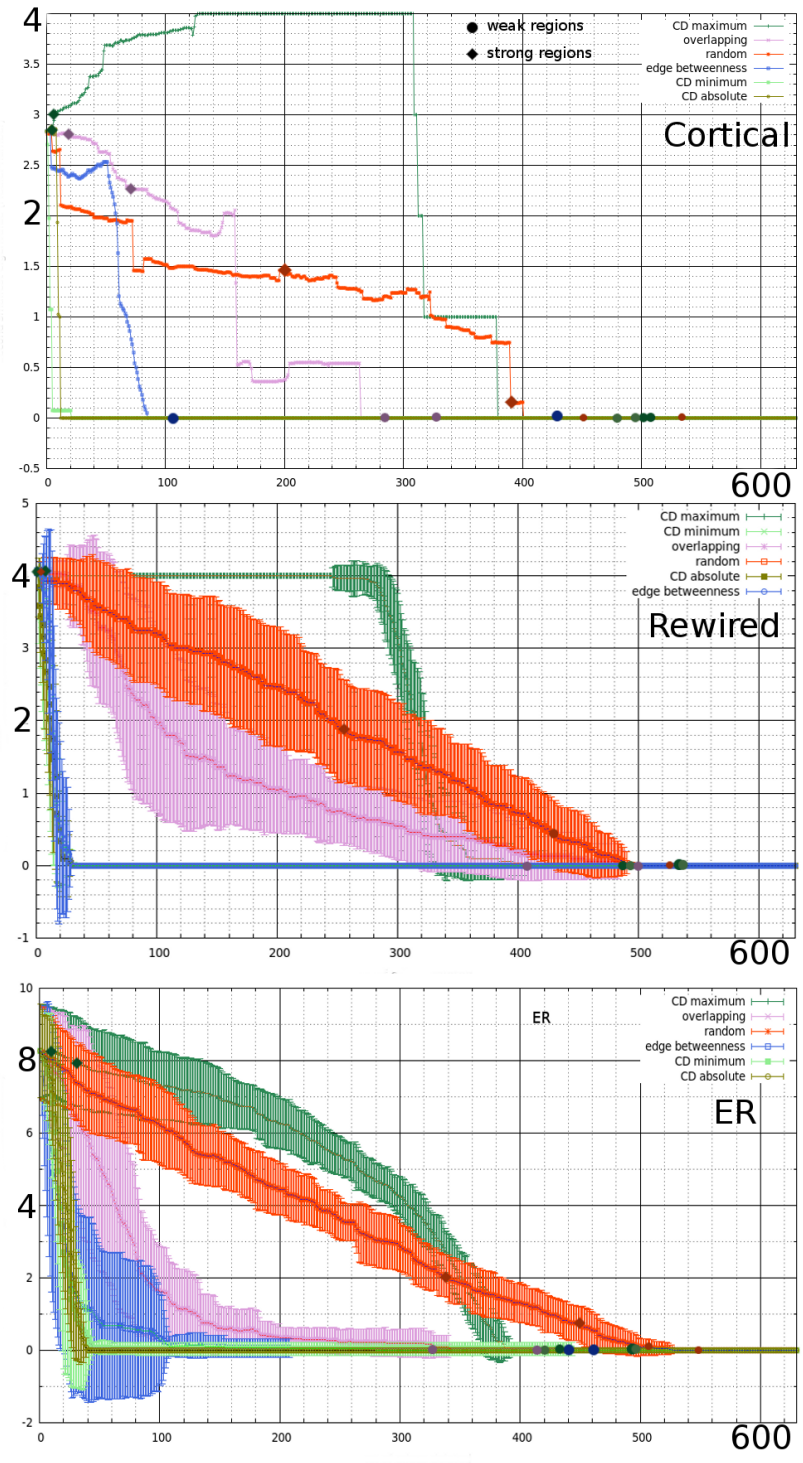

***Figure 14.** The algebraic connectivity in the function of the nr. of edges removed by different attack strategies [Key 1.]*

In the cortical and rewired networks Overlapping target was closer in behavior to the random target than in the ER networks. This suppose the higher resilience of the recurrent pathways of the connectedness in cortical-like networks, because its target behaves like a random removing. On the contrary the EB based target was more λ_2^{real} vulnerable in the rewired networks, but not in the

macaque. Initially the cortical and rewired networks had edges with higher EB values [Fig 1.], removing them can cause bigger damage.

Convergent, i.e. CD max, edge target had a similar effect in both random types, if we look at the ER deleting after $\lambda_2^{real}<4$ [Fig. 14.]. In the macaque an increase can be seen in λ_2^{real} at convergent edge removes, which is contrary to what's known about undirected graphs. A consistent $\lambda_2^{real}=4$ region without deviation is present during convergent edge elimination in the rewired network, and it is also present in the macaque network and must be a specific value of λ_2^{real}, since that is the values λ_2^{real} show the “prohibited” increase.

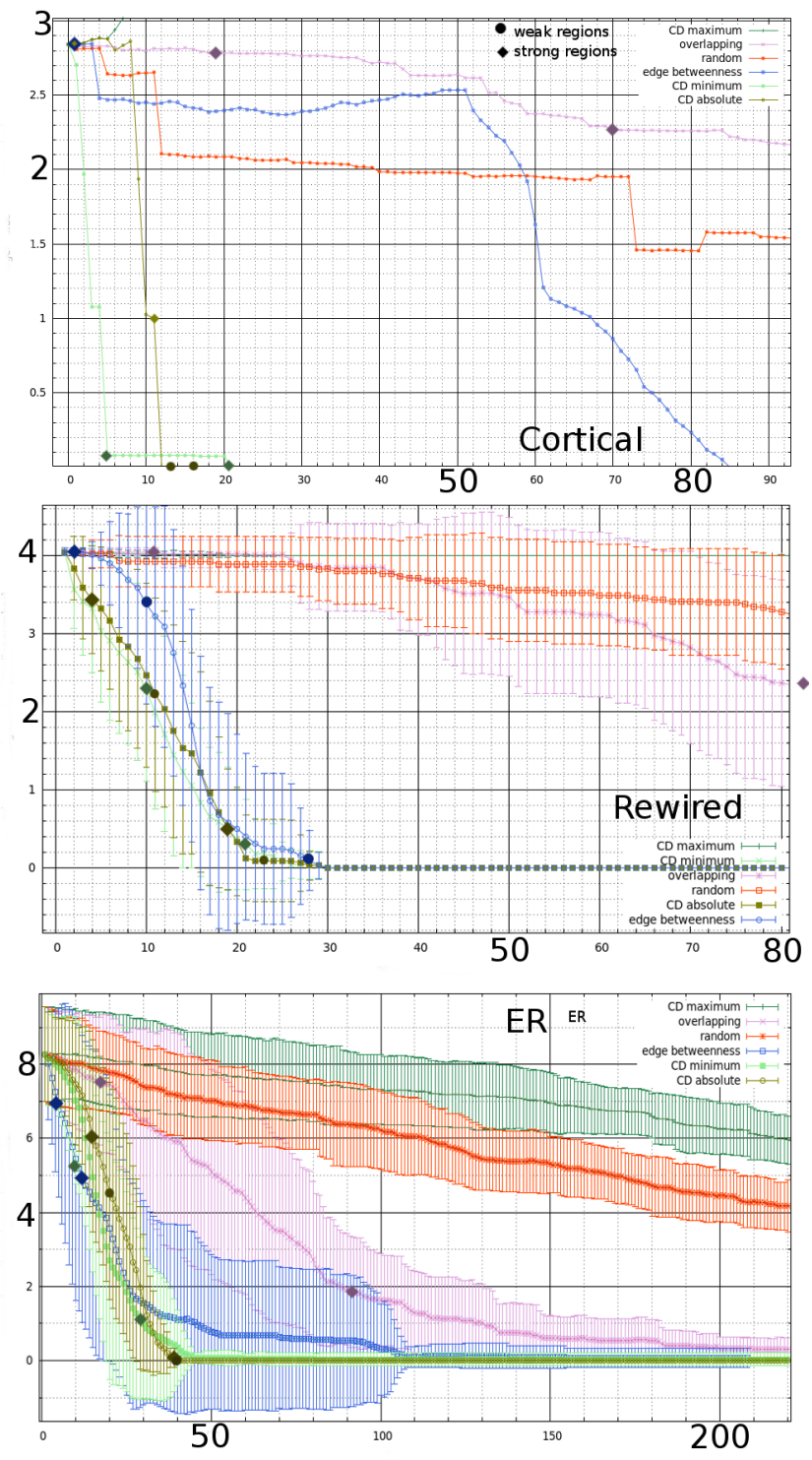

Figure 15. *The algebraic connectivity in the function of the nr. of edges removed by different attac strategies [Key 1.] at the first part of the removing process*

λ_2 *relation to connected components*

To determine the relation of the undirected λ_2 and the connectivity on the spectral vulnerability graphics the number of connected components are noted with the beginnings and with the ends of regions, where 1.06<nr. of connected components<2.06 [Table 6. and Table 7.]. Cycles note if it is weak, squares if it is a strong disconnected components [Fig. 14 and Fig. 15]. In the case of the macaque network the signs denote the region where the nr. of connected components exactly 2.

All networks were vulnerable to the absolute CD target, its strong and weak disconnecting regions were somewhat overlapping, suggesting the immediate weak disconnecting after the strong disconnect. This is also confirmed with the similar steepness of the nr. of strong/weak connected components [Fig. 12. and Fig. 11.]. Overall at CD absolute target the connectivity correlated well with λ_2^{real} reaching 0 [Fig. 15].

At Overlapping based and random targets the region strong disconnecting is expanded,

implying their random behavior on the directed disconnecting, also generally with these targets λ_2^{real} reached 0 close or in the region of the weak (total) disconnecting.

Signed CD remove show similar regions for both signs to strong and weak separations, they separates strongly at the beginning of the attack, and disconnects fully at the end phase, but λ_2^{real} had very different acts depending on if convergent or divergent edges gets removed. λ_2^{real} decrease fast if divergent edges got removed, while the network stays weakly connected until the end of the deletion. Removing divergent edges at first will decrease the algebraic connectivity slowly in ER and converge to 4 at the cortical degree distribution [Fig. 14.]. After removing around half of the edges will λ_2^{real} have a steep fall. This suggest, that λ_2^{real} above the connectivity properties of the network might include properties about the signal propagation, e.g. divergence.

For all targets the regions of strong (one-directional) disconnectedness and the $\lambda_2=0$ comes later in ER then in the rewired networks ($\lambda_2=0$ is with the exception of the Overlapping and convergent edge target). The later decrease of λ_2 and the slower disconnecting can be in relation with the higher λ_2^{real} values. Higher λ_2 suppose a better connected structure, where more edges needs to be removed from to disconnect the graph. Though, this was not holding to the weak (total) disconnecting regions, suggesting the importance of directed connectedness in the magnitude of λ_2^{real}.

The strongly disconnecting regions of the cortical are fitting in its rewired randomized regions. In the strong disconnecting there is no sign of the deviant EB behavior, but the weak disconnecting region shows the difference, it comes later than in the rewired network with conserved degree-distribution. This might suggests a degree sequence independent resilience of the cortical network to busy connections with high EB.

The eigenratio

The maximal value the eigenratio, λ_2/λ_{max} can take is 1, means an even spectrum, indicating a

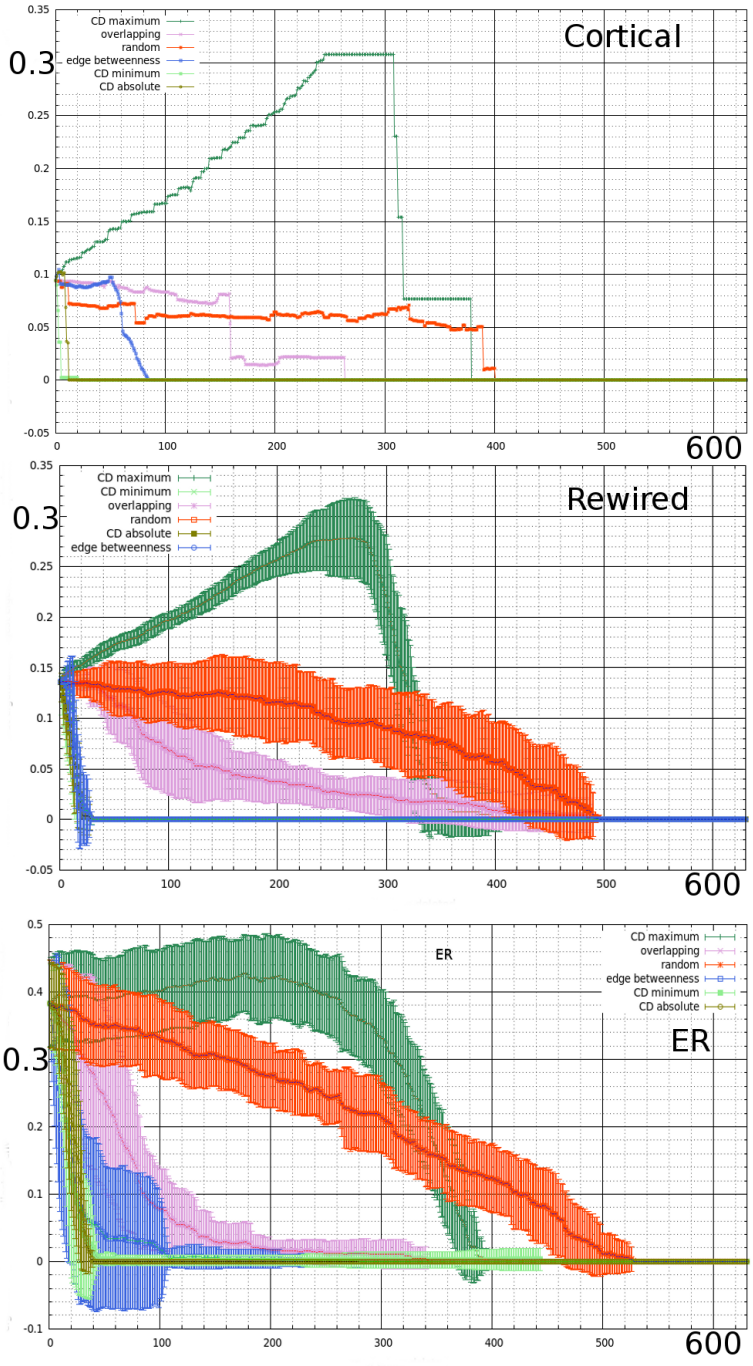

Figure 16. *The eigenratio (second smallest eigenvalue devided by the larges eigenvalue) in the function of the nr. of edges removed at different attack strategies [Key 1.]*

stable synchronization manifold. The eigneratio becomes zero when λ_2.

The behavior [Fig. 16.] of the ratio resembles very well to what was seen at λ_2 [Fig. 14], but pronounced increase can be seen in the eigenratio at all types of networks during convergent edge remove, suggesting the role of divergent edges in the support of synchronization. The increase is much pronounced in the rewired networks, though it had initially lower λ_2/λ_{max} [Table 2.].

If edges removed with the maximum CD, then the proportion of edges converging signals decrease, information disperse routes increase. Since then an average signal can reach higher amount of nodes, a signal going trough an edge have higher influence on other nodes. The bigger influence nodes have on each other, the advanced the synchronizability is. If spreading edges gets deleted, the number of convergent connections increase, passing signals got sunk in these, making it though to synchronize nodes, and explanation what can be made to the high eigenratio vulnerability of the divergent target [Fig. 16.].

Effects on the largest eigenvalue

The strongest effect on the means of decreasing the largest eigenvalue was by the CD maximum target, which was specially pronounced by the cortical rewired network [Fig. 17.]. Meanwhile divergent and overlapping target had little effect on decreasing λ_{max}. An interesting difference in the behavior by the EB target could be seen between the cortical rewired and the ER network, the cortical rewired network seem to show vulnerability, while in the ER random graph EB target had little effect in the decrease of the largest eigenvalue.

Changes in the steepness can be seen at several target bias, like high steepness, small steepness regions coming alternately, e.g. in maximal CD, EB, minimal CD and Overlapping targets, but often in a different manner. Interestingly, random edge elimination was similar to the absolute CD target by lacking this change in steepness and giving a similar rate of decresing in λ_{max}.

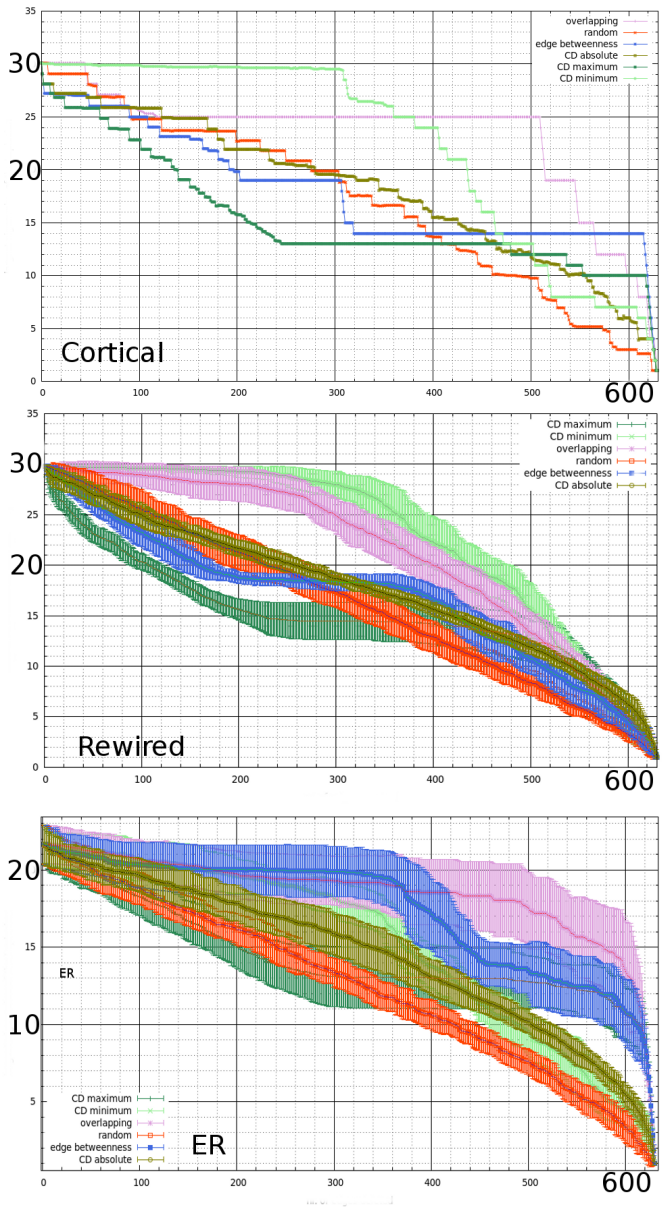

Figure 17. *The largest eigenvalue of the Laplacian in the function of the nr. of edges removed by different attack strategies [Key 1.]*

Conclusions

Network properties

Compared to the ER network a more clustered structure of the rewired, and cortical network can be derived from the higher ASP and CC values, also more heterogeneity by the edge values, like EB and CDs can be stated. The smaller Overlapping values, and that the network reaching the overlapping-free state sooner indicates less recurrent connections in the network. Less connected structure is also assumed from the edge values and the algebraic connectivity.

The cortical network showed prominent differences mostly in the smaller algebraic connectivity values.

Higher amount of divergent edges were also pointed out, meaning the moderate predominance of Feed-Forward connections in the brain, as the cortical degree distribution holds the difference in convergent and divergent edge properties. Higher amount of divergent edges is assumed to be present after the negative average CD of the initial network and after the more divergent edges needed to remove to reach the zero average CD. The highest valued convergent and divergent edges removed had very similar absolute value, and with knowing the heterogeneity of convergent/divergent edges in the cortical networks, the higher amount of divergent edges, and not edges with higher negative convergence degree are assumed. Divergent edges identified as the feed-forward connections in the cortical hierarchy, thus the the increased nr. of FF connections can be stated.

Centralities

Edge betweenness was shown again to be a good target of vulnerability, specially in increasing the average shortest paths and to separate the graph to strongly connected components.

Convergence Degree derived measures were specially vulnerable targets in some instances, where other measures, like EB, were otherwise less efficient. Absolute CD target was prominently effective in weakly separating a network and increasing the Clustering Coefficient.

Both CD absolute and minimum (divergent edge) targets were highly efficient to reduce the algebraic connectivity, while CD maximal (convergent) edge target had the special effect of increasing the quantity.

In the first pars of the edge deletion processes Overlapping was not a specially efficient target, in most cases networks were resilient against it, but interestingly at later periods network vulnerability measures, e.g. strong connectivity showed a phase-transition-like behavior with fast, strong effects. Indicates, that network are resilient to remove Overlapping, recurrent, pathways, but removing almost all routes like that cause big harm to the network structure.

Topologies

While the directed ER graphs, with the same amount of nodes and edges, showed symmetrical properties for both negative and positive CD based deletion, the cortical network were more vulnerable to convergent edge deletion. Those are mostly the feed-back connections integrating information from higher order areas, playing an important role in the signal processing.

Heterogeneous CD values and the smaller Overlapping in the rewired network indicated a

more directed information processing and a more hierarchical organization.

The rewired network was more sensitive to EB and CD based targets compared to ER, which might be due to the heterogeneity of these values in the network.

Some properties of the cortical network are connected to the degree distribution, like the higher clustering and the eigenvalues are also seemed to be constrained by the degree distribution. The higher average shortest path and the less connected structure trough the algebraic connectivity of the cortical network is supposed to be derived from the spatial constrains, i.e. the spatial embeddedness of the network.

Robustness, synchronizability and spectral properties

The decrease of λ_2^{real} shows correlation with the network disconnecting, but it is depending on the target edge property. In the randomized networks for random edge removes generally the network disconnected in one direction when λ_2^{real} was small enough (~ λ_2^{real} <2), and λ_2^{real} became zero in the weakly disconnecting region. Similar behavior was seen at Overlapping target as well, but with strong disconnecting sooner, i.e. at higher λ_2^{real} values. Note that these targets don't contain divergence properties, so their effect on λ_2^{real} might correlate well with connectivity features because it fails to pronounce the effects on divergence.

λ_2^{real} was very vulnerable and its decrease is correlated very well to disconnecting at CD absolute target. With removing negative and positive high CD edges, also divergent edges got removed, along with injuring connectivity effectively, thus resulting the correlation to disconnecting and fast decrease of λ_2^{real}.

In some instances, 4 seem to be a characteristic value of λ_2^{real}, since removing convergent edges from a network with initial λ_2^{real} smaller and bigger than 4 will result the convergence of λ_2^{real} to 4. This also implies the possibility to increase the real value of the directed algebraic connectivity by removing edges if the graph is directed, which is not allowed in undirected graphs. From the pronouncedly different behavior of λ_2^{real} to convergent and divergent edge removes, the directed algebraic connectivity can be concluded to contain path divergence properties of the network, besides the properties of the connectivity.

A directed graph can have non-zero λ_2^{real} and be disconnected bi-directionally as well, pronouncing the differing eigenvalue meanings from the ones derived from the undirected spectral analyses.

The ER was found to be the easiest to synchronize, the most suitable to hold stable synchronization from the three examined networks by the eigenratios. This moreover fits to the needs of the cortical networks since the brain rather need to hold transient and partial synchronizations.

References:

[1] P Holme, BJ Kim, CN Yoon, SK Han - Physical Review E, 2002, Attack vulnerability of complex networks

[2] CJ Keller, CJ Honey, P Mégevand- Phil. Trans. R, 2014, Mapping human brain networks with cortico-cortical evoked potentials

[3] PJ Uhlhaas, C Haenschel, D Nikolić, W Singer - Schizophrenia bulletin, 2008, The role of oscillations and synchrony in cortical networks and their putative relevance for the pathophysiology of schizophrenia

[4] M Bányai, L Négyessy, F Bazsó - Journal of Statistical Mechanics, 2011, Organization of signal flow in directed networks

[5] J Luo, CL Magee - Complexity, 2011, Detecting evolving patterns of self-organizing networks by flow hierarchy measurement

[6] L Négyessy, T Nepusz - Royal, 2008, Convergence and divergence are mostly reciprocated properties of the connections in the network of cortical areas

[7] A Arenas, A Díaz-Guilera, J Kurths, Y Moreno, C Zhou - Physics reports, 2008, Synchronization in complex networks

[8] P Fries - Trends in cognitive sciences, 2005, A mechanism for cognitive dynamics: neuronal communication through neuronal coherence

[9] S Boccaletti, V Latora, Y Moreno, M Chavez - Physics reports, 2006, Complex networks: Structure and dynamics

[10] M Fiedler - Czechoslovak mathematical journal, 1973, Algebraic connectivity of graphs

[11] M Kaiser, CC Hilgetag - Biological cybernetics, 2004, Edge vulnerability in neural and metabolic networks

[12] R Yuste - Nature Reviews Neuroscience, 2015, From the neuron doctrine to neural networks

[13] VB Mountcastle - Brain, 1997 - Oxford Univ Press, The columnar organization of the neocortex

[14] E Bullmore, O Sporns - Nature Reviews Neuroscience, 2009, Complex brain networks: graph theoretical analysis of structural and functional systems

[15] P Uhlhaas, G Pipa, B Lima, L Melloni - Frontiers in, 2009, Neural synchrony in cortical networks: history, concept and current status

[16] XJ Wang, H Kennedy - Current opinion in neurobiology, 2016, Brain structure and dynamics across scales: in search of rules

[17] D Bavelier, HJ Neville - Nature Reviews Neuroscience, 2002, Cross-modal plasticity: where and how?

[18] NT Markov, H Kennedy - Current opinion in neurobiology, 2013, The importance of being hierarchical

[19] MEJ Newman - The new palgrave encyclopedia of economics, 2008, The mathematics of networks

[20] E Mones, L Vicsek, T Vicsek - PloS one, 2012, Hierarchy measure for complex networks

[21] AE Motter, C Zhou, J Kurths - Physical Review E, 2005, Network synchronization, diffusion, and the paradox of heterogeneity

[22] Jessell T, Kandel E, Siegelbaum S, Schwartz J, Hudspeth A.J. (2012) Principles of Neural Science. Fifth Edition. McGraw-Hill

[23] Bullock TH, Bennett MV, Johnston D, Josephson R, Marder E, Fields RD. Neuroscience. The neuron doctrine, redux. Science. 2005 310(5749):791-3.

[24] Bastos AM, Usrey WM, Adams RA, Mangun GR, Fries P, Friston KJ. Canonical microcircuits for predictive coding. Neuron. 2012; 76(4):695- 711.

[25] Kaas JH. Evolution of columns, modules, and domains in the neocortex of primates. Proc

Natl Acad Sci U S A. 2012; 109 Suppl 1:10655-60.

[26] Olaf Sporns (2007) Brain connectivity. Scholarpedia, 2(10):4695.

[27] Cole MW, Bassett DS, Power JD, Braver TS, Petersen SE. Intrinsic and task-evoked network architectures of the human brain. Neuron. 2014; 83(1):238-51.

[28] Mišić B, Sporns O. From regions to connections and networks: new bridges between brain and behavior. Curr Opin Neurobiol. 2016; 40:1-7.

[29] Lanciego JL, Wouterlood FG. A half century of experimental neuroanatomical tracing. J Chem Neuroanat. 2011; 42(3):157-83.

[30] Bullmore E, Sporns O. The economy of brain network organization. Nat Rev Neurosci. 2012; 13;13(5):336-49.

[31] Felleman DJ, Van Essen DC. Distributed hierarchical processing in the primate cerebral cortex. Cereb Cortex. 1991; 1(1):1-47.

[32] Markov NT, Ercsey- Ravasz M, Van Essen DC, Knoblauch K, Toroczkai Z, Kennedy H. Cortical high-density counterstream architectures. Science. 2013; 342(6158):1238406.

[33] Schmolesky MT, Wang Y, Hanes DP, Thompson KG, Leutgeb S, Schall JD, Leventhal AG. Signal timing across the macaque visual system. J Neurophysiol. 1998 79(6):3272-8.

[34] Hochstein S, Ahissar M. View from the top: hierarchies and reverse hierarchies in the visual system. Neuron. 2002 Dec 5;36(5):791-804.

[35] Lennie P. Single units and visual cortical organization. Perception. 1998; 27(8):889-935.

[36] Hochstein S, Ahissar M. View from the top: hierarchies and reverse hierarchies in the visual system. Neuron. 2002 Dec 5;36(5):791-804.

[37] Shipp S. Neural Elements for Predictive Coding. Front Psychol. 2016; 7:1792.

[38] Friston K. The free-energy principle: a unified brain theory? Nat Rev Neurosci. 2010 11(2):127-38.

[39] Buzsáki G, Draguhn A. Neuronal oscillations in cortical networks. Science. 2004; 304(5679):1926-9.

[40] Buzsáki G, Anastassiou CA, Koch C. The origin of extracellular fields and currents--EEG, ECoG, LFP and spikes. Nat Rev Neurosci. 2012; 13(6):407-20.

[41] Toldi J. Representational plasticity in the mammalian brain cortex. (Review article). Acta Physiol Hung. 2008; 95(3):229-45.

[42] Tononi G, Edelman GM, Sporns O. Complexity and coherency: integrating information in the brain. Trends Cogn Sci. 1998; 2(12):474-84.

[43] R Mason A. Porter (2012) Small-world network. Scholarpedia, 7(2):1739.

[44] Olaf Sporns (2007) Complexity. Scholarpedia, 2(10):1623.

[45] Softky and Koch, 1993; The highly irregular firing of cortical cells is inconsistent with temporal integration of random EPSPs

[46] DS Bassett, ED Bullmore - The neuroscientist, 2006, Small-World Brain Networks